DEPARTMENT OF THE INTERIOR

U.S. GEOLOGICAL SURVEY

Differential Displacements and Differential Spectra for the February 20, 1988 Hollister, California, earthquake

by

G. N. Bycroft and P. N. Mork[1]

Open-File Report No. 88-679

[1] Menlo Park, California

Differential Displacements and Differential Spectra for the February 20, 1988 Hollister Earthquake

G. N. Bycroft and P. N. Mork

Abstract

Differential ground motion under the base of a structure imposes direct strain on the structure in addition to the strains caused by inertial loading. In order to assess the importance of these differential strains, differential arrays of digital accelerometers with pre-event memory were installed at El Centro and Hollister, California. These arrays produced useful data for the 1979 El Centro, the 1984 Morgan Hill, the 1981 Westmorland, and the 1986 and 1988 Hollister earthquakes in California. This report presents differential displacements and spectra for the ML = 5.3 1988 Hollister earthquake of February 20, 0839 G.M.T. The differential displacements and spectra for the first 4 earthquakes are discussed in Bycroft and Mork, 1987. In certain circumstances the differential strains are significant.

Introduction

Aseismic design generally has assumed that all points on the ground move in unison with the free-field motion over a region that is larger than the foundation of the structure. This assumption is based on the notion that seismic waves are propagated substantially in high-wave-velocity basement rock and transmitted vertically to the region of interest through lower velocity layers. However, surface waves propagating horizontally through surface layers may have wavelengths along the surface of approximately the dimensions of a large structure (Trifunac, 1972; Wong and Trifunac, 1974; Bycroft, 1980). Further, differential ground motion may be caused by local inhomogeneity. The foundation of the structure would then undergo differential motions that would cause additional strains to be superimposed on those due to inertial loading. Thus, for example, adjacent bridge piers would move relative to each other and cause stresses in the piers and the bridge decking. Structures built on spread footings, dams and pipelines would be similarly affected.

To study such motion, differential ground motions must be measured. Methods of utilizing this information in seismic design should be developed. Arrays of seismometers have been installed at El Centro and Hollister, California. These arrays are discussed in Bycroft (1982, 1983). Figure 1 shows the configuration of the Hollister array.

Differential Displacments

The processing of accelerograms to give displacements has long been a problem due to the double integrations of base-line error, long-period noise quantification errors, and problems related to the mechanics of film transport. The original processing was directed towards digitized film records and was developed initially at the California Institute of Technology. Many changes have been made at the U.S.G.S. resulting in a present form known as AGRAM (Converse, 1984). This program has many options available depending on the judgement of the user for his particular application or data. The processing includes instrument corrections, base line corrections and high pass filtering to eliminate long period noise and quantification errors.

In studying the direct strains on a structure displacements themselves are of no interest because only the difference of displacements occur in the structural equations. Consequently, only differential displacements are considered. This difference will eliminate those real long-period seismic signals whose wavelengths are large compared to the spacing of the stations.

Differential Spectra

In order to examine the significance of a structure subjected to differential strain loading in addition to the inertial loading, a simple model, that is affected by both these loadings was investigated. Figure 2 shows this structure as a simple single-span bridge structure with two vertical piers connected by a deck. Transverse horizontal ground motions are applied to this structure so that shear stresses are developed in the three components. The masses are lumped together where the deck joins the piers. The masses are equal to **m**, the shear stiffness of the piers is $\mathbf{k}_1$ and the shear stiffness of the deck is $\mathbf{k}_2$. Different horizontal displacements $y_1(t)$ and $y_2(t)$ are applied to the base of each pier. A response spectrum **R** was calculated. This response spectrum is defined as the ratio of the maximum strain in pier 1 when the displacement inputs are $y_1(t)$ and $y_2(t)$ to that of the maximum strain in pier 1 when $y_1(t) = y_2(t)$. This ratio R is then a suitable measure of the effect of the addition of differential strain to the inertial loading. It is readily shown that

(1) $$R = \frac{A}{B}$$

where

(2) $$A = \frac{Max}{2} \int_o^t C \, d\tau$$

where Max means the maximum value of the integral during the length of the input and where

(3) $$C = \frac{e^{-\lambda\omega_1 (t-\tau)} \{\ddot{y}_1(\tau) + \ddot{y}_2(\tau)\} \sin \omega_1 (t-\tau)}{\omega_1} \frac{+e^{-\lambda\sqrt{\omega_1{}^2+2\omega_2^2}\,(t-\tau)} [\ddot{y}_1(\tau) - \ddot{y}_2(\tau) + 2\omega_2^2 \{y_1(\tau) - y_2(\tau)\}] \sin\left[\sqrt{\omega_1^2+2\omega_2^2}\,(t-\tau)\right]}{\sqrt{\omega_1{}^2+2\omega_2{}^2}}$$

(4) $$B = \frac{Max \int_o^t e^{-\lambda\omega_1 (t-\tau)} \ddot{y}_1(\tau) [\sin \omega_1 (t-\tau)] \, d\tau}{\omega_1}$$

(5) $\omega_1 = \sqrt{\frac{k_1}{m}}$

(6) $\omega_2 = \sqrt{\frac{k_2}{m}}$

(7) λ = modal damping factor, common to both modes.

Similar equations apply to the longitudinal horizontal motions.

These spectra are for a simple two-degree-of-freedom structure and are relevant to situations where the two stations are close. A multi-degree-of-freedom spectra is being developed that is more relevant to stations farther apart.

February 20, 1988 Hollister Records

The Hollister Differential Array gave useful data from stations 1, 2, 5, and 6 for the February 20, 1988 Hollister earthquake.

Differential Displacements

The double integration of accelerograms that give satisfactory values of differential displacements is discussed in Bycroft and Mork (1987a). Again, a bidirectional Butterworth filter with a long period cut-off of 5 seconds and order 2 was used. The base line correction was determined by least square fitting a zero line through the first 2 sec. of each record. The displacements at stations 5 and 6 were rotated to give displacements longitudinal and transverse to the joining leg. Figs. 3, 4, 5, and 6 show the corrected accelerograms and the differential displacements between the stations 2 and 1, 6 and 1, 5 and 1, and 6 and 5 for the first 20 seconds. This was a small earthquake and the difference of displacements is correspondingly small.

Differential Spectra

Differential spectra have been calculated from equation 1 and are shown in figs. 7 through 30 for various parameter values. For low values of omega 1 the value of R tends to a value close to unity. For high values of omega 1 the value R is significantly higher than 1 showing that differential strains are now quite significant. In the intermediate range of omega 1 the value of R is significantly lower than 1 in most but not all cases. This is different from the earthquakes discussed in Bycroft and Mork (1987a and 1987b) and could be a function of the locations of the epicenters relative to that of the array. The effect of damping shown for the cases omega 1 equals omega 2 does not follow any recognizable trend.

Conclusions

Differential displacements contribute significantly to the strains developed in larger structures by an earthquake especially for the higher frequencies. Different earthquakes, recorded at the same array, show significantly different trends in the mid range of frequency presumably because of the different location of the epicenters. In general, no distinct patterns are discernable in the current data and consequently much more data from many different locations and earthquakes is needed.

References

Bycroft, G.N., 1980, Soil foundation interaction and differential ground motions: Journal of Earthquake Engineering and Structural Dynamics, v. 8, no. 5, p. 397-404.

Bycroft, G.N., 1982, El Centro differential ground motion array: U.S. Geological Survey Professional Paper 1254, p. 351-356.

Bycroft, G.N., 1983, Differential ground motion array at Hollister Municipal Airport, California: U.S. Geological Survey Open-File Report No. 83-327.

Bycroft, G.N. and P.N. Mork (1987a), Differential displacements and differential spectra for April 26, 1981 Westmorland and the January 26, 1986 Hollister earthquakes: U.S. Geological survey Open-File Report 87-62.

Bycroft, G.N., and P.N. Mork (1987b), Differential spectra for the 1979 El Centro and the 1984 Morgan Hill earthquakes: U.S. Geological Survey Open-File Report 87-94.

Converse, A.M., 1984, AGRAM: A series of computer programs for processing digitized strong-motion accelerograms, version 2.0: U.S. Geological Survey Open File Report 84-525, 118 p.

Trifunac, M.D., 1972, Interaction of a shear wall with the soil for incident plane SH waves: Seismological Society of America Bulletin, v. 62, no. 1, p. 63-83.

Wong, H.L., and Trifunac, M.D., 1974, Interaction of a shear wall with the soil for incident plane SH waves: Elliptical rigid foundation: Seismological Society of America Bulletin, v. 64, no. 6., p. 1825-1842.

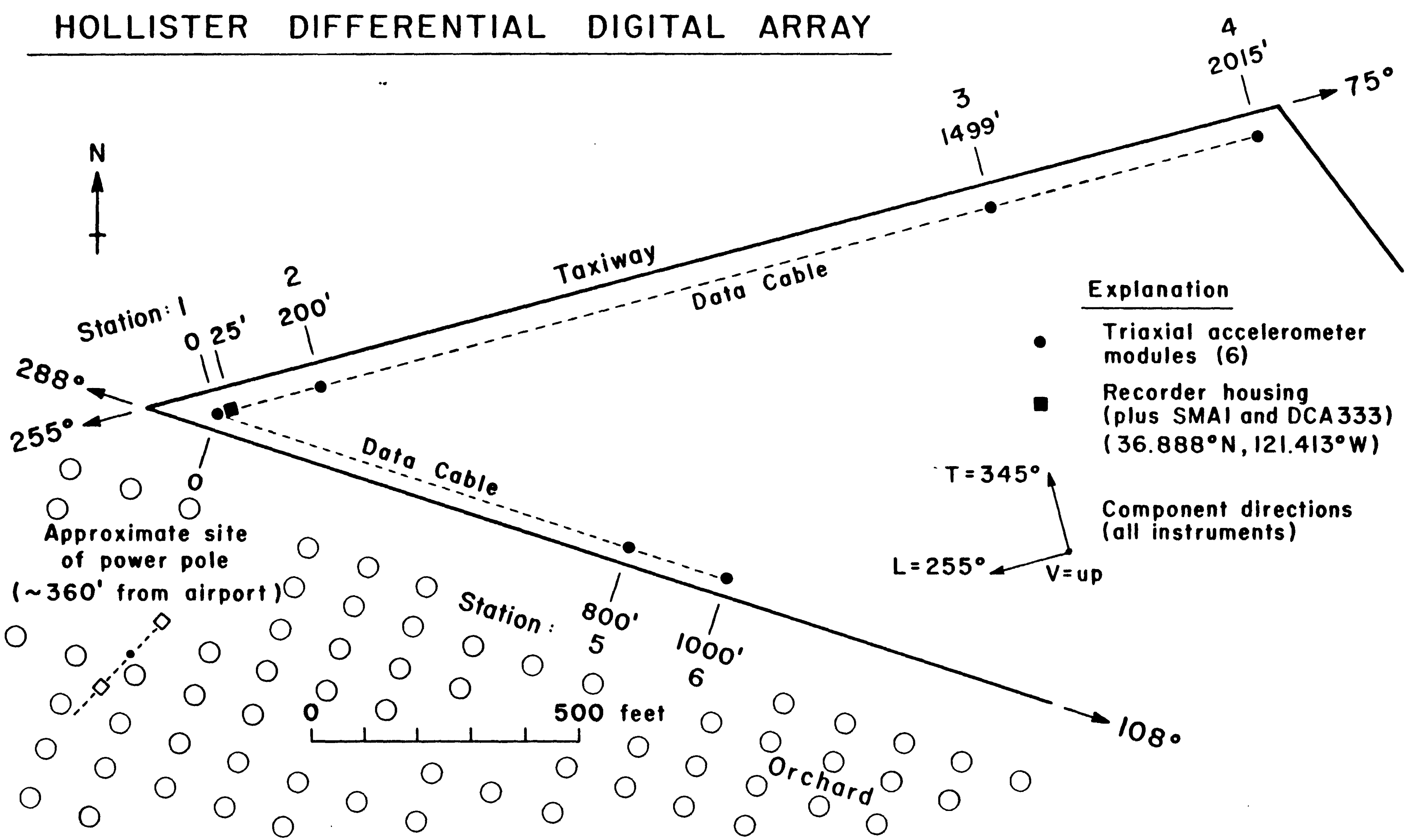
HOLLISTER DIFFERENTIAL DIGITAL ARRAY
N
Taxiway
Data Cable
Data Cable
Station: 1
0 25'
2
200'
3
1499'
4
2015'
75°
288°
255°
108°
0
Station:
800'
5
1000'
6
Approximate site
of power pole
(~360' from airport)
0
500 feet
Orchard
Explanation
Triaxial accelerometer modules (6)
Recorder housing
(plus SMA1 and DCA333)
(36.888°N, 121.413°W)
T=345°
L=255°
V=up
Component directions
(all instruments)

FIGURE 1

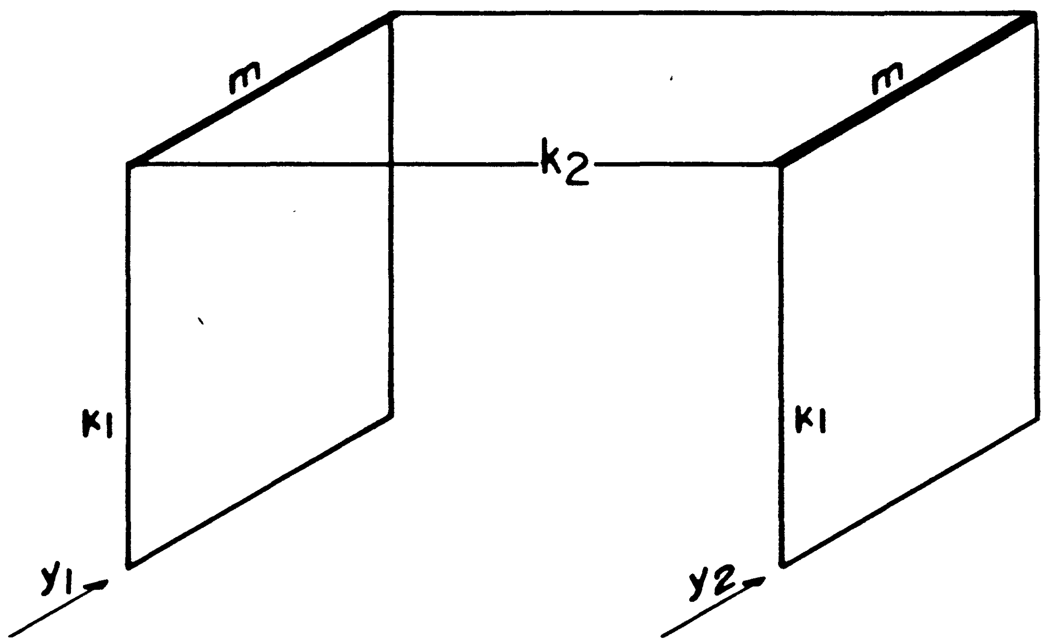

Figure 2. Model for differential spectra.

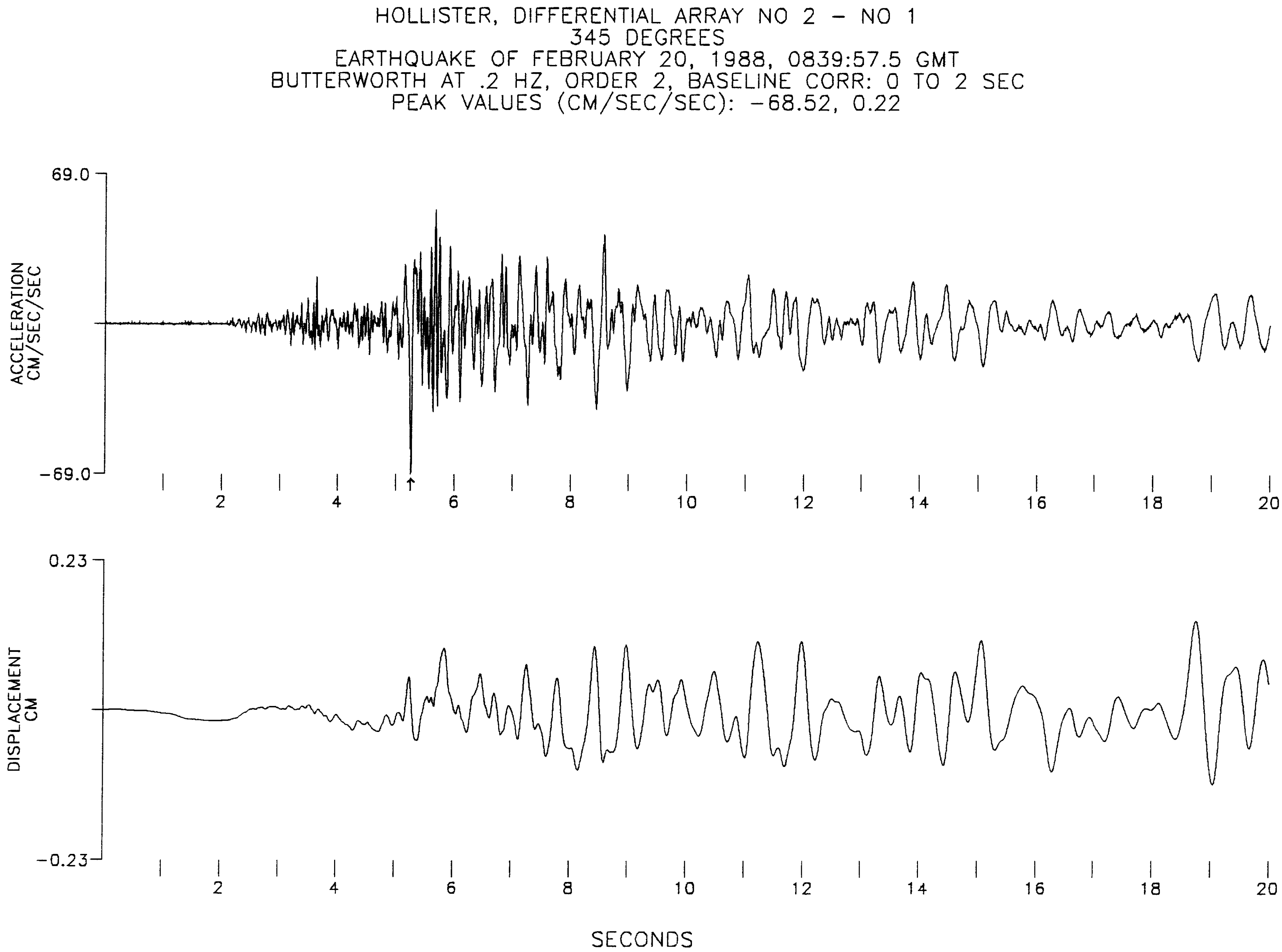
HOLLISTER, DIFFERENTIAL ARRAY NO 2 – NO 1
345 DEGREES
EARTHQUAKE OF FEBRUARY 20, 1988, 0839:57.5 GMT
BUTTERWORTH AT .2 HZ, ORDER 2, BASELINE CORR: 0 TO 2 SEC
PEAK VALUES (CM/SEC/SEC): –68.52, 0.22
ACCELERATION CM/SEC/SEC
69.0
–69.0
DISPLACEMENT CM
0.23
–0.23
2
4
6
8
10
12
14
16
18
20
SECONDS

Fig 3

HOLLISTER, DIFFERENTIAL ARRAY NO 6 – NO 1, ROTATED
018 DEGREES
EARTHQUAKE OF FEBRUARY 20, 1988, 0839:57.5 GMT
BUTTERWORTH AT .2 HZ, ORDER 2, BASELINE CORR: 0 TO 2 SEC
PEAK VALUES (CM/SEC/SEC): –222.51, –0.61

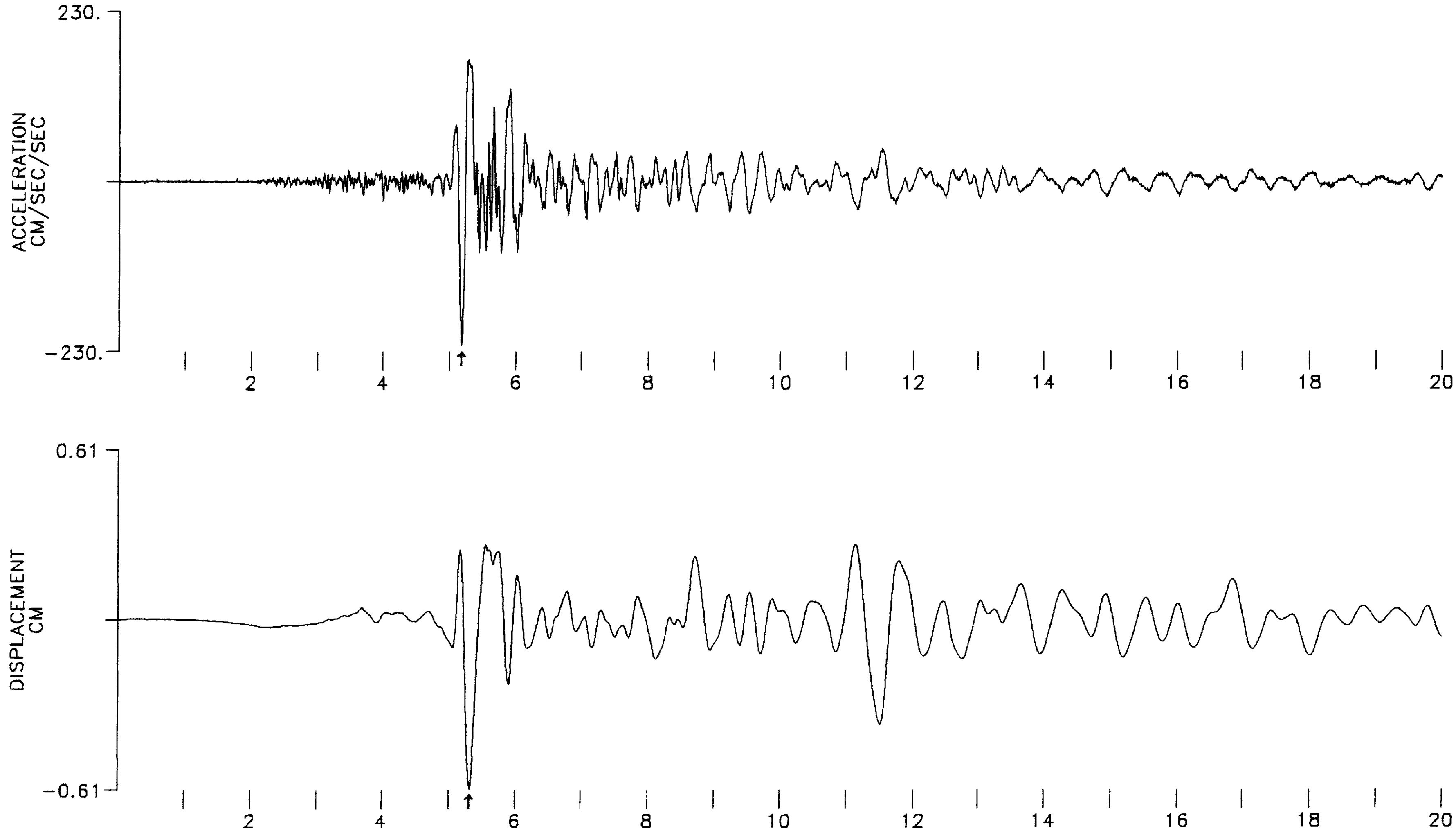

Fig 4

HOLLISTER, DIFFERENTIAL ARRAY NO 5 – NO 1, ROTATED
018 DEGREES
EARTHQUAKE OF FEBRUARY 20, 1988, 0839:57.5 GMT
BUTTERWORTH AT .2 HZ, ORDER 2, BASELINE CORR: 0 TO 2 SEC
PEAK VALUES (CM/SEC/SEC): –162.94, –0.22

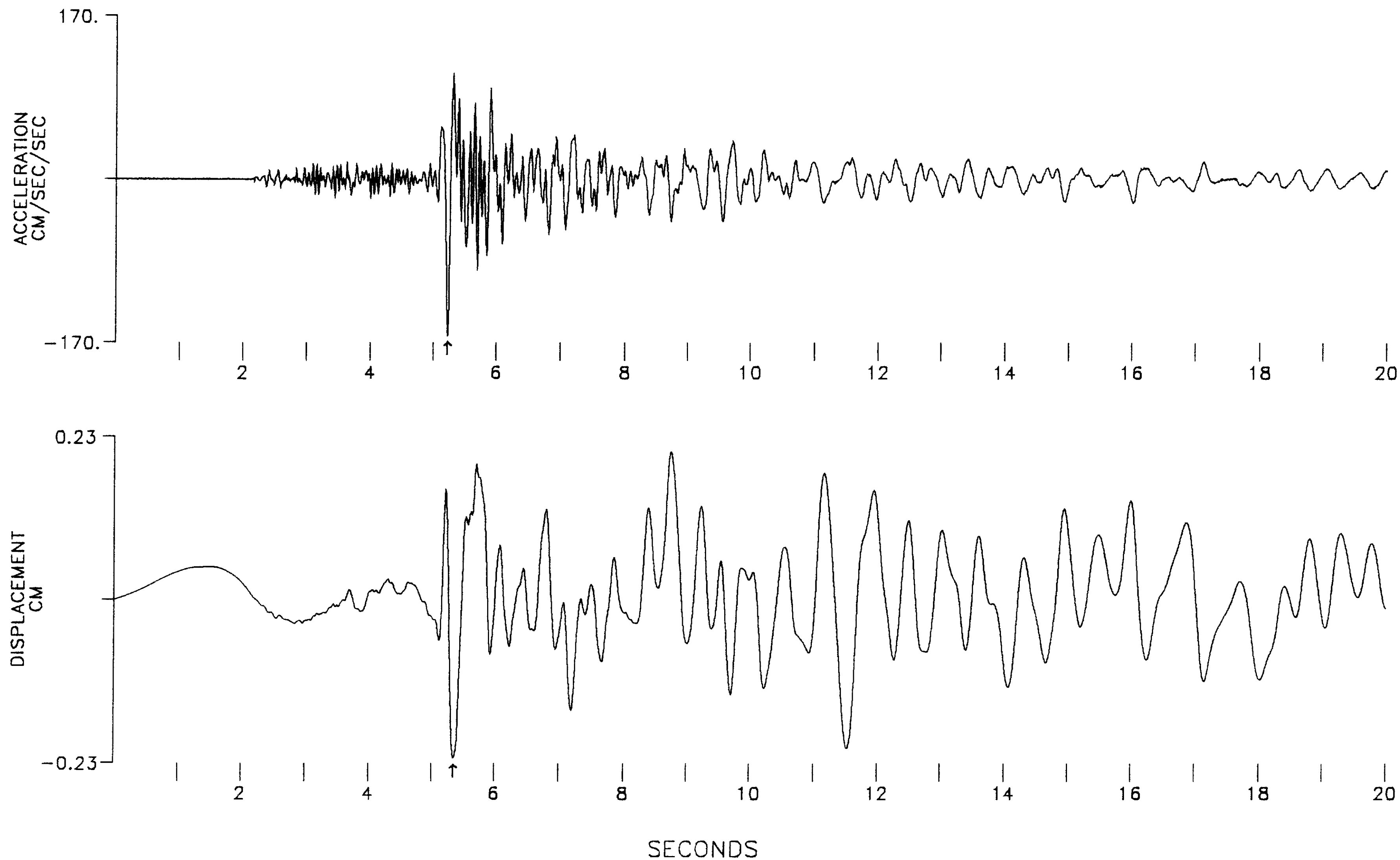

Fig 5

HOLLISTER, DIFFERENTIAL ARRAY NO 6 – NO 5, ROTATED
018 DEGREES
EARTHQUAKE OF FEBRUARY 20, 1988, 0839:57.5 GMT
BUTTERWORTH AT .2 HZ, ORDER 2, BASELINE CORR: 0 TO 2 SEC
PEAK VALUES (CM/SEC/SEC): −238.60, −0.46

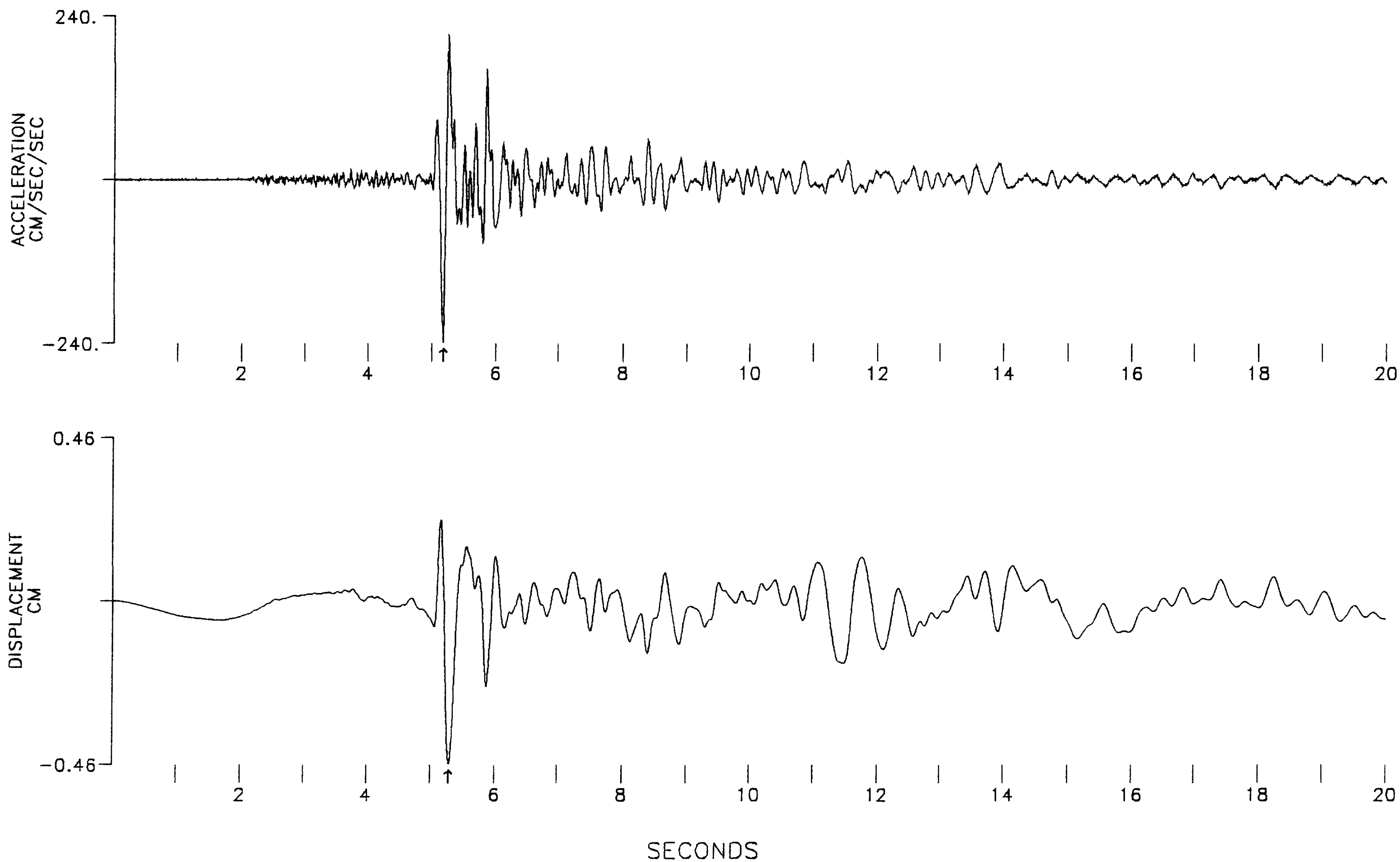

Fig 6

HDIFF2-HDIFF1, ØMEGA 2 = ØMEGA 1 DAMPING = 0.0, LENGTH = 30. SEC, CHANNEL 03

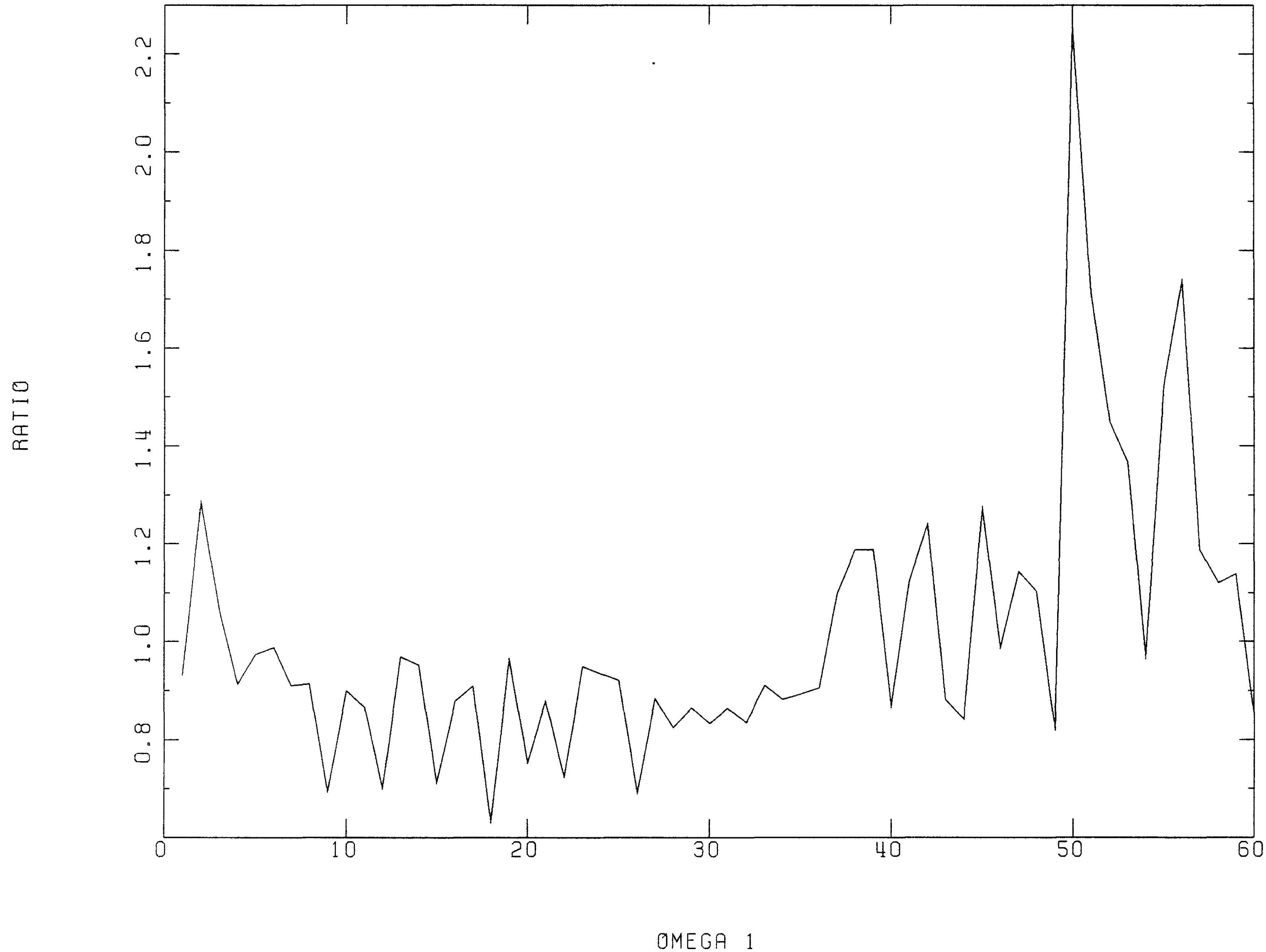

Fig 7

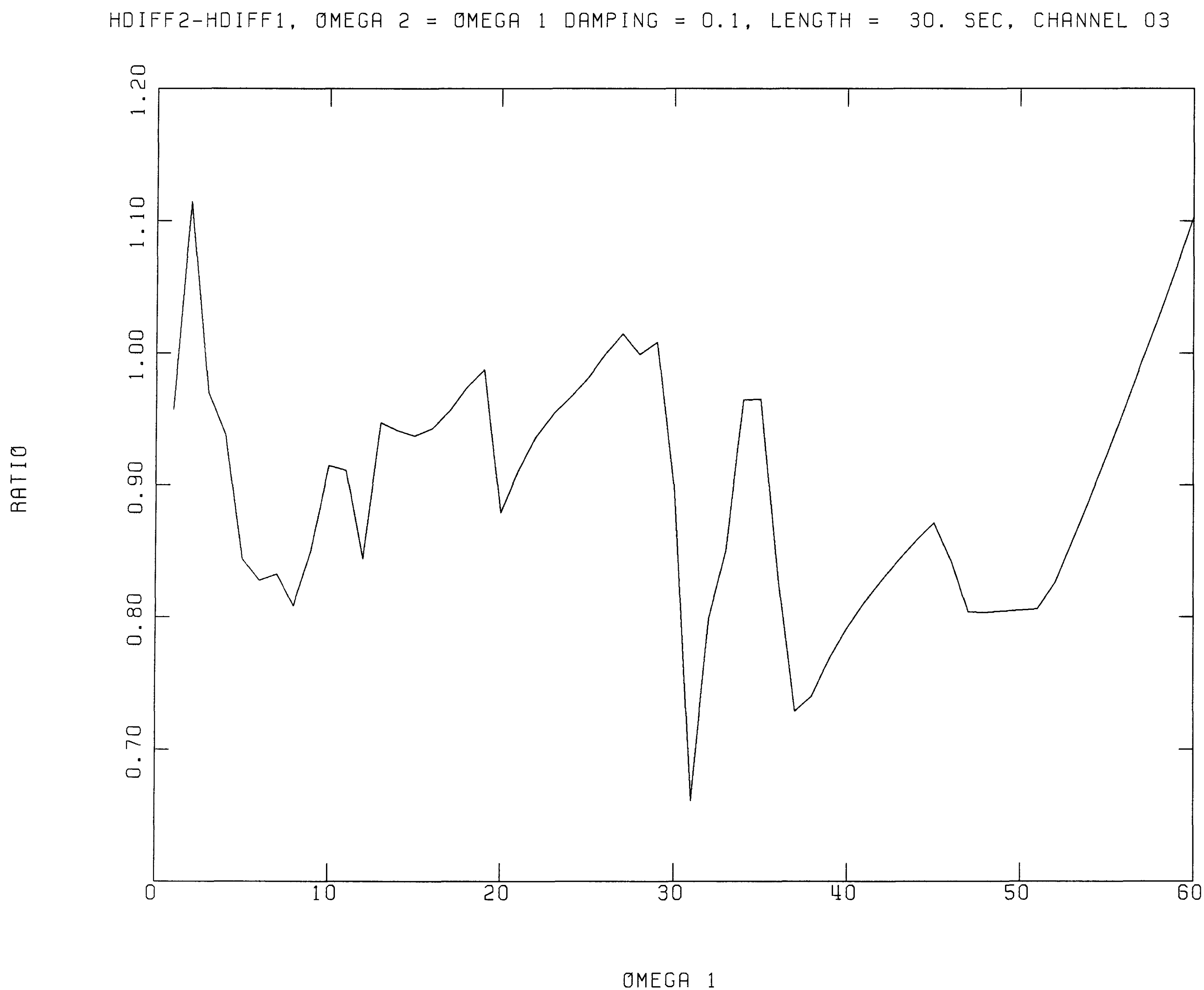
HDIFF2-HDIFF1, ØMEGA 2 = ØMEGA 1 DAMPING = 0.1, LENGTH = 30. SEC, CHANNEL 03
RATIØ
1.20
1.10
1.00
0.90
0.80
0.70
0
10
20
30
40
50
60
ØMEGA 1

Fig 8

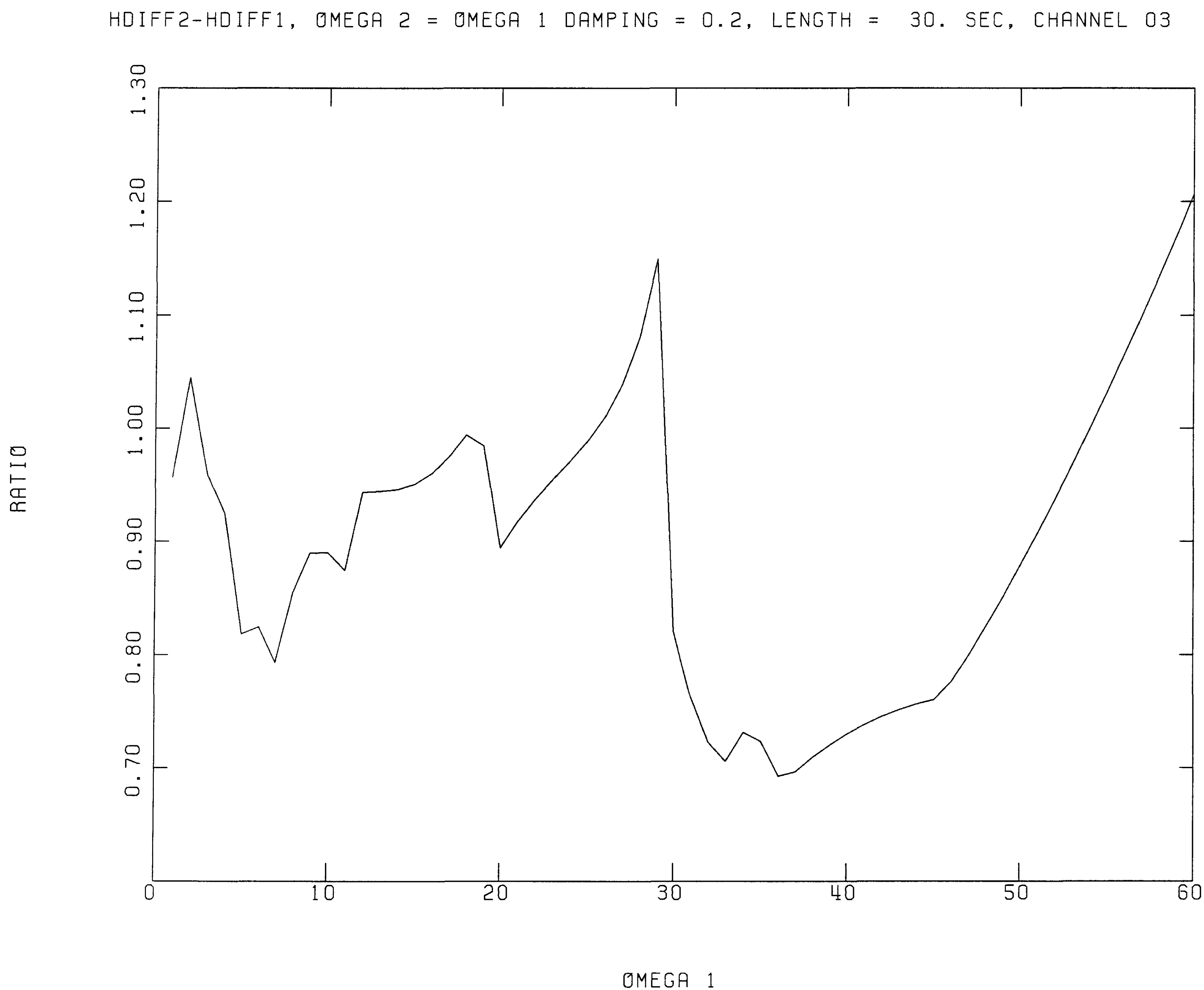
HDIFF2-HDIFF1, ØMEGA 2 = ØMEGA 1 DAMPING = 0.2, LENGTH = 30. SEC, CHANNEL 03
RATIØ
1.30
1.20
1.10
1.00
0.90
0.80
0.70
0
10
20
30
40
50
60
ØMEGA 1

Fig 9

HDIFF2-HDIFF1, ØMEGA 2 = 10.0 DAMPING = 0.0, LENGTH = 30. SEC, CHANNEL 03

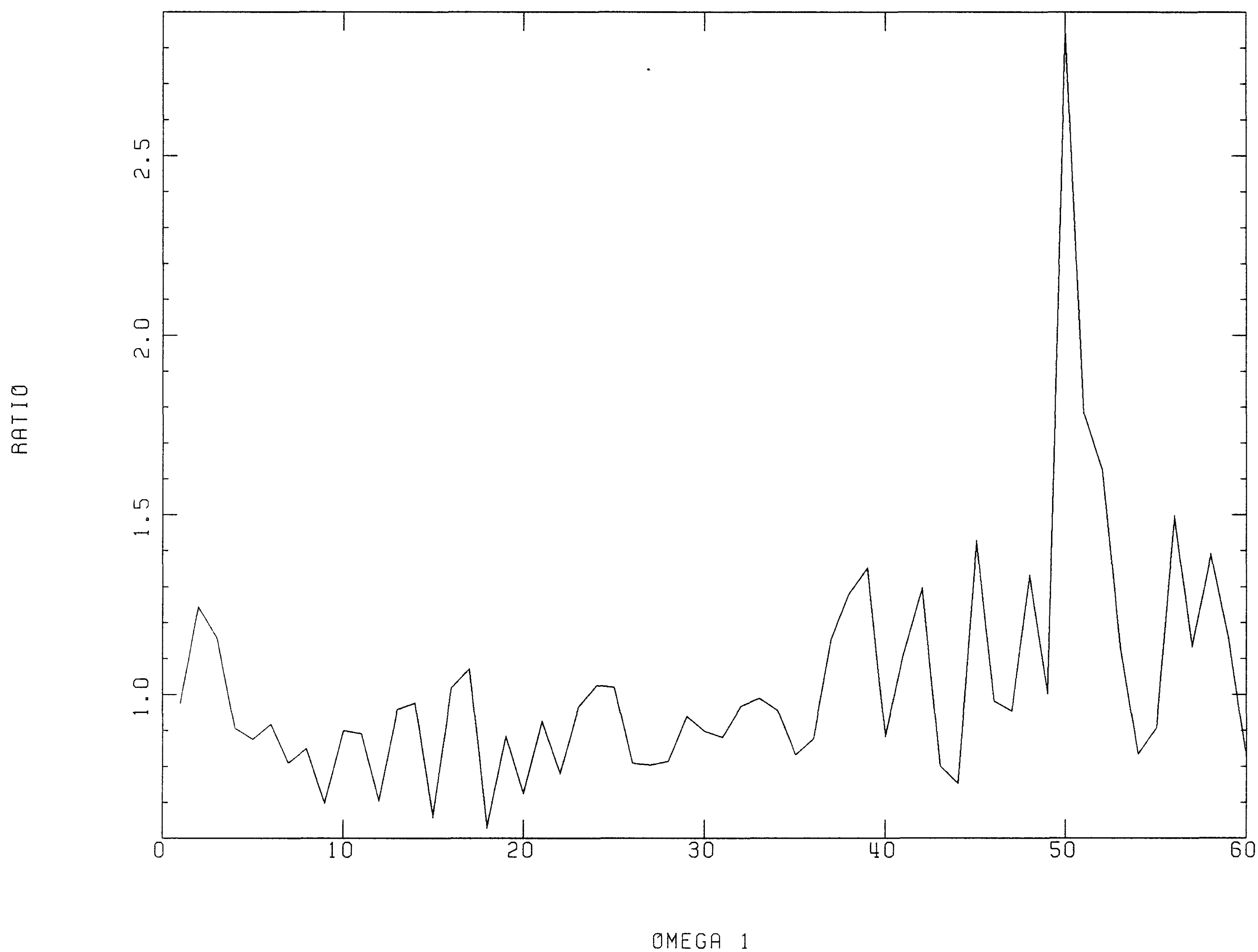

Fig 10

HDIFF2-HDIFF1, ØMEGA 2 = 30.0 DAMPING = 0.0, LENGTH = 30. SEC, CHANNEL 03

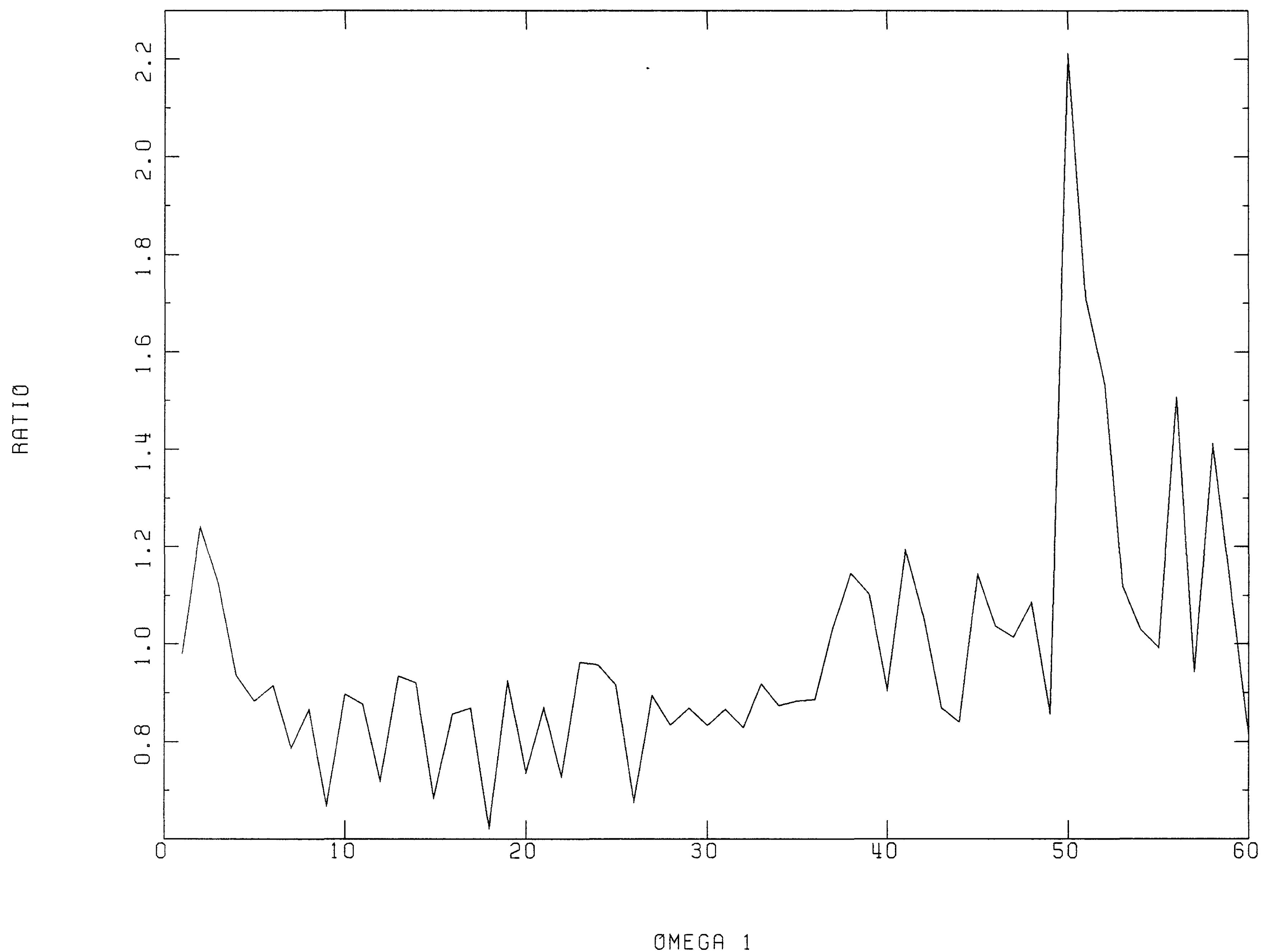

Fig 11

HDIFF2-HDIFF1, ØMEGA 2 = 50.0 DAMPING = 0.0, LENGTH = 30. SEC, CHANNEL 03

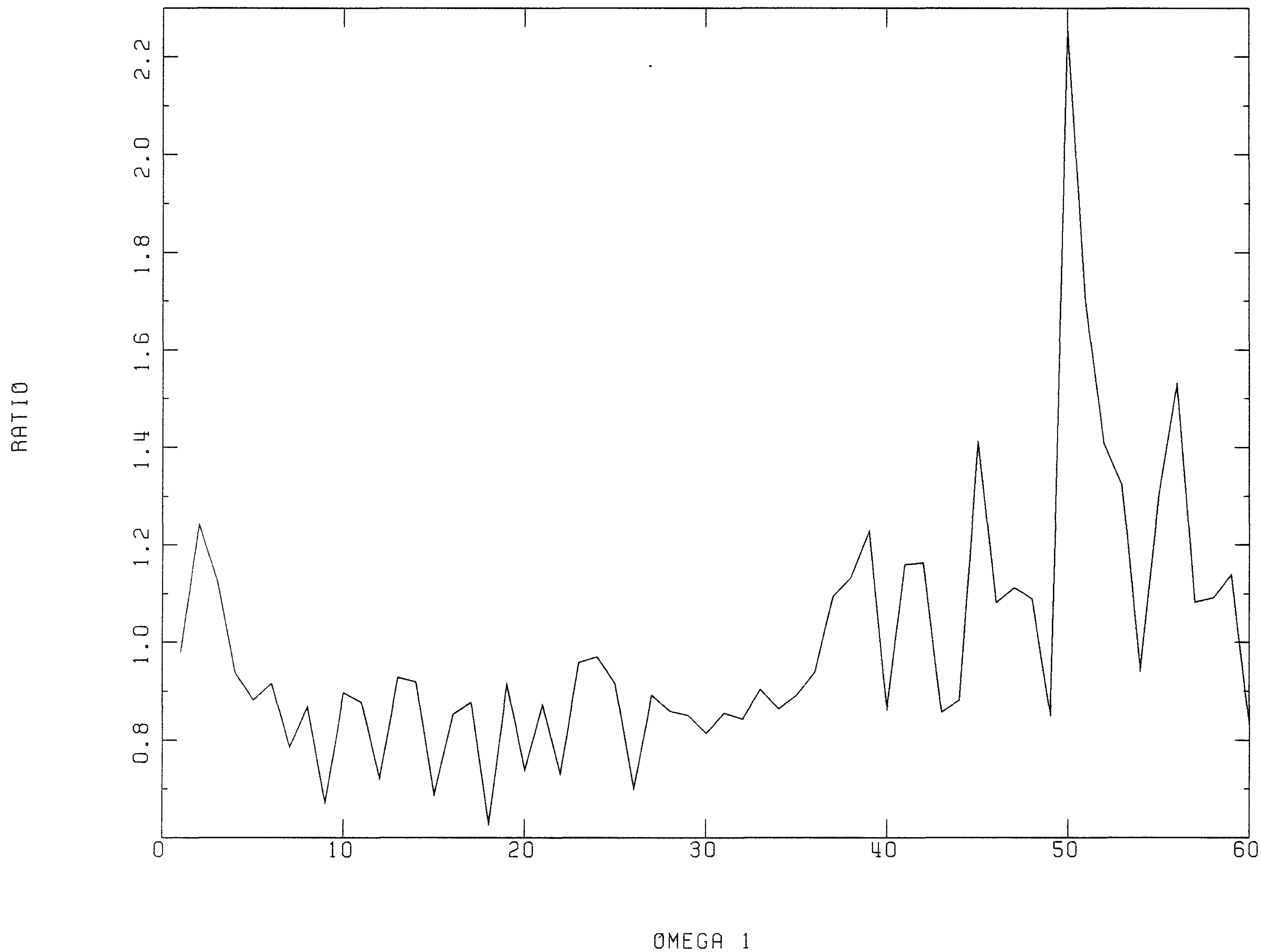

Fig 12

RHDIFF6-RHDIFF1, ØMEGA 2 = ØMEGA 1 DAMPING = 0.0, LENGTH = 30. SEC, CHANNEL 03

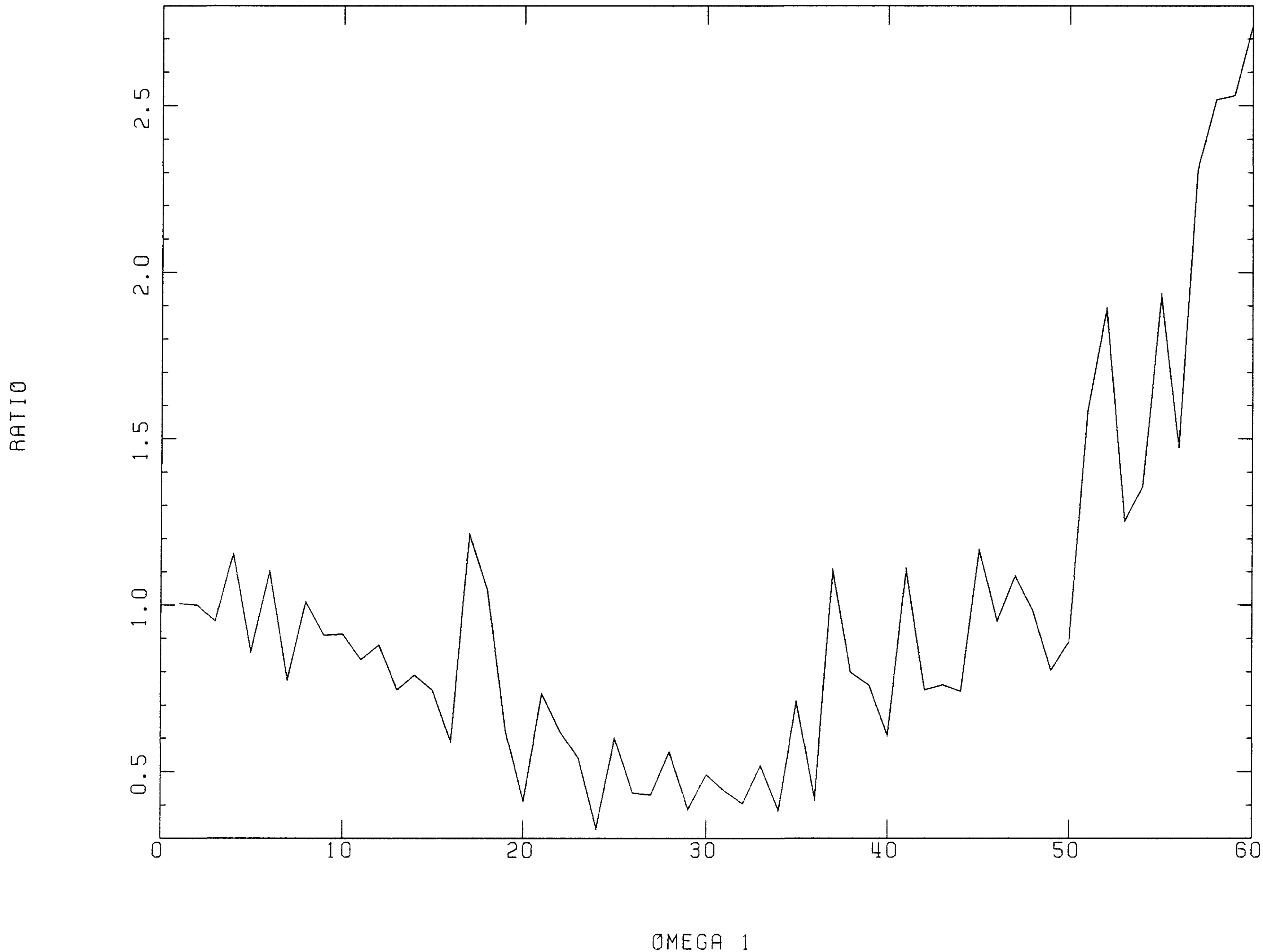

Fig 13

RHDIFF6-RHDIFF1, ØMEGA 2 = ØMEGA 1 DAMPING = 0.1, LENGTH = 30. SEC, CHANNEL 03

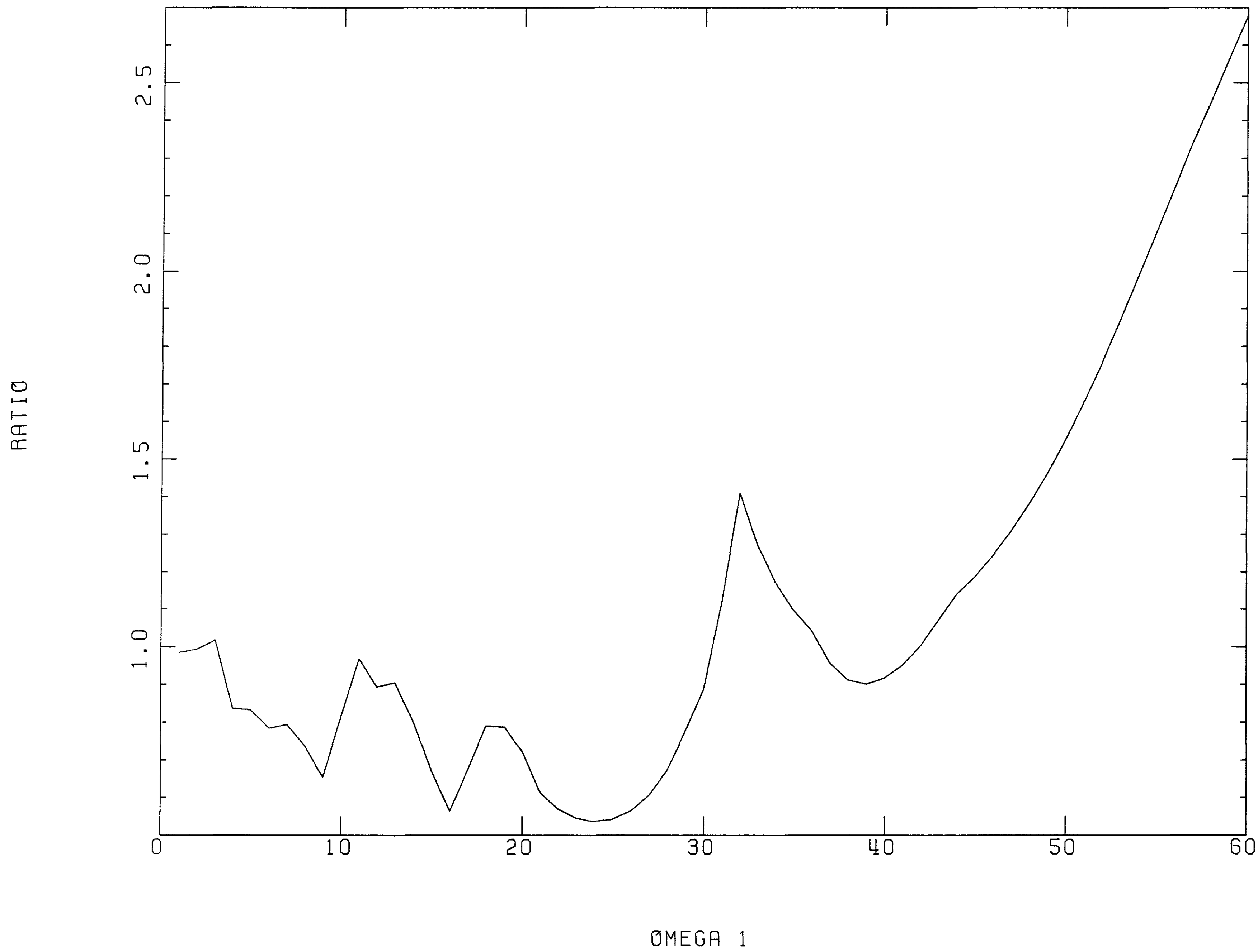

Fig 14

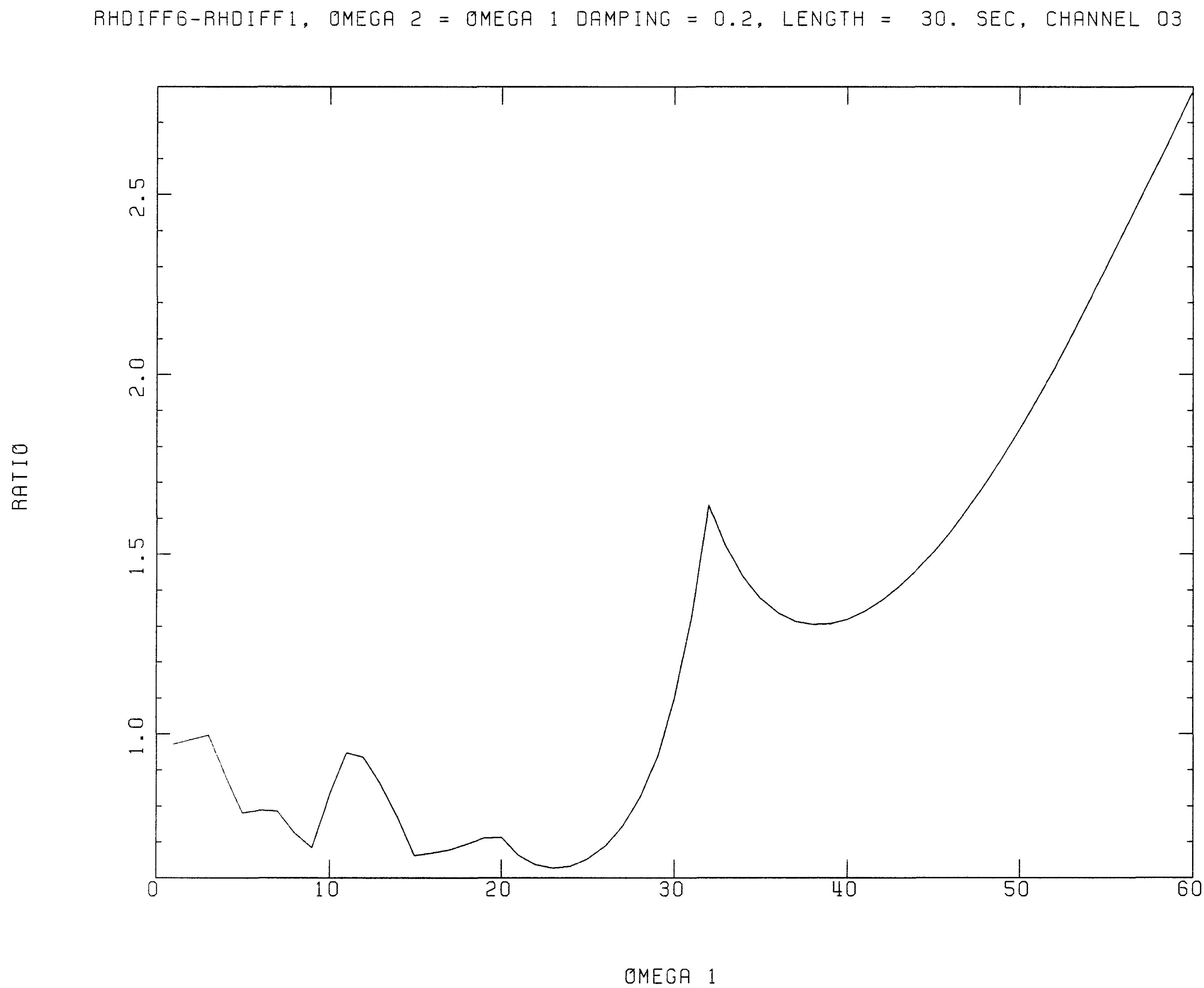
RHDIFF6-RHDIFF1, ØMEGA 2 = ØMEGA 1 DAMPING = 0.2, LENGTH = 30. SEC, CHANNEL 03
RATIØ
2.5
2.0
1.5
1.0
0
10
20
30
40
50
60
ØMEGA 1

Fig 15

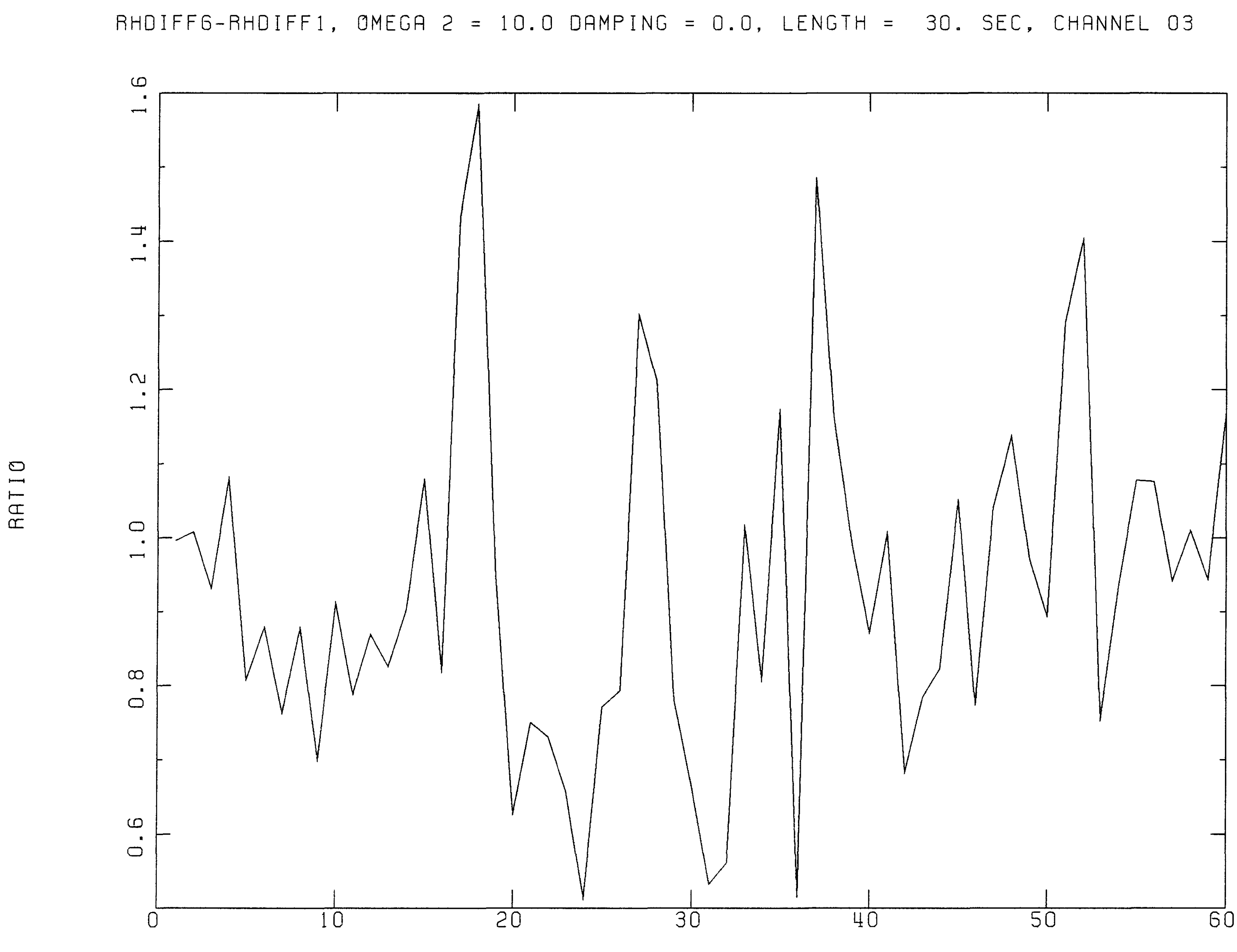
RHDIFF6-RHDIFF1, ØMEGA 2 = 10.0 DAMPING = 0.0, LENGTH = 30. SEC, CHANNEL 03
RATIØ
1.6
1.4
1.2
1.0
0.8
0.6
0
10
20
30
40
50
60
ØMEGA 1

Fig 16

RHDIFF6-RHDIFF1, ØMEGA 2 = 30.0 DAMPING = 0.0, LENGTH = 30. SEC, CHANNEL 03

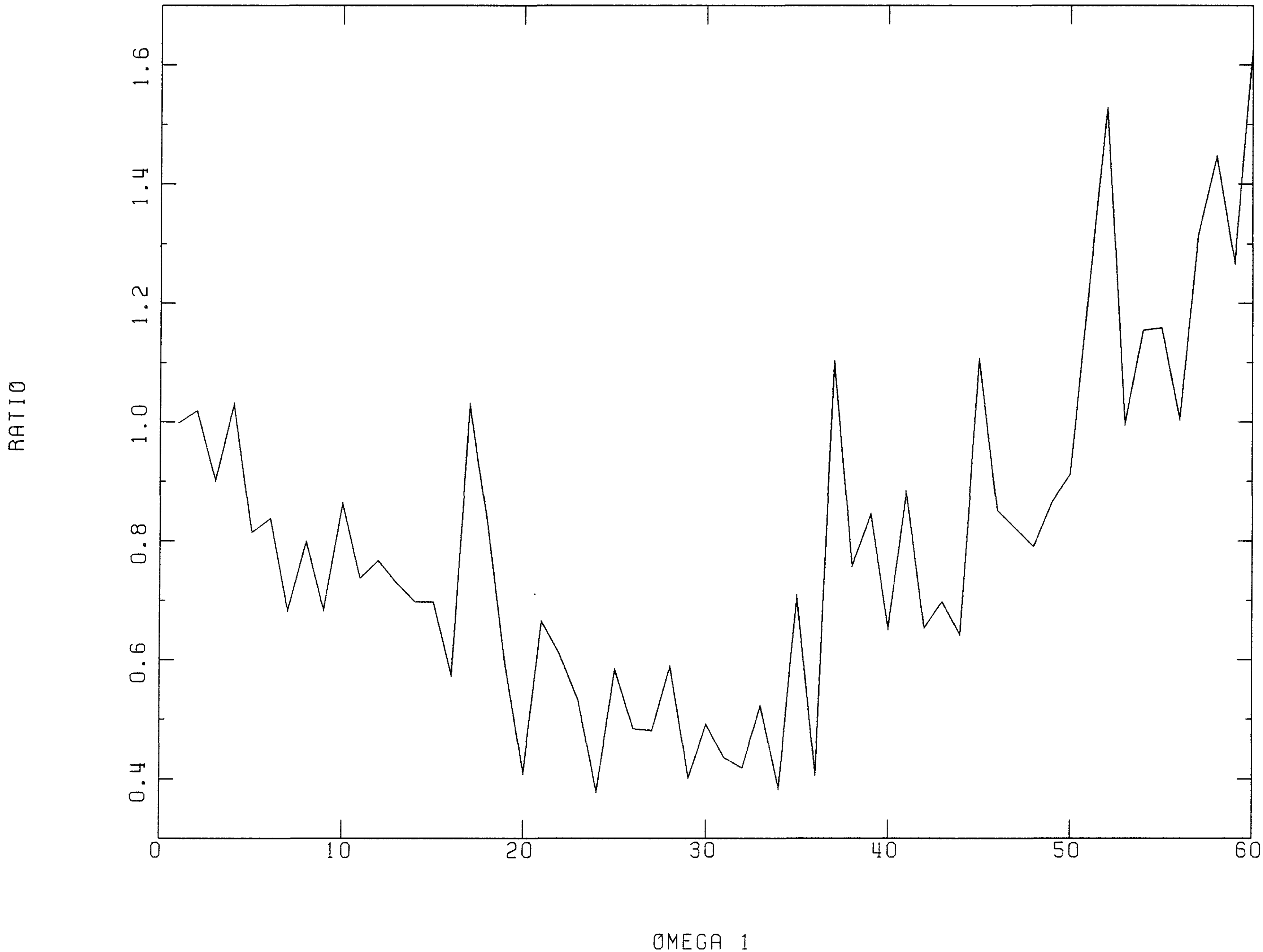

Fig 17

RHDIFF6-RHDIFF1, ØMEGA 2 = 50.0 DAMPING = 0.0, LENGTH = 30. SEC, CHANNEL 03

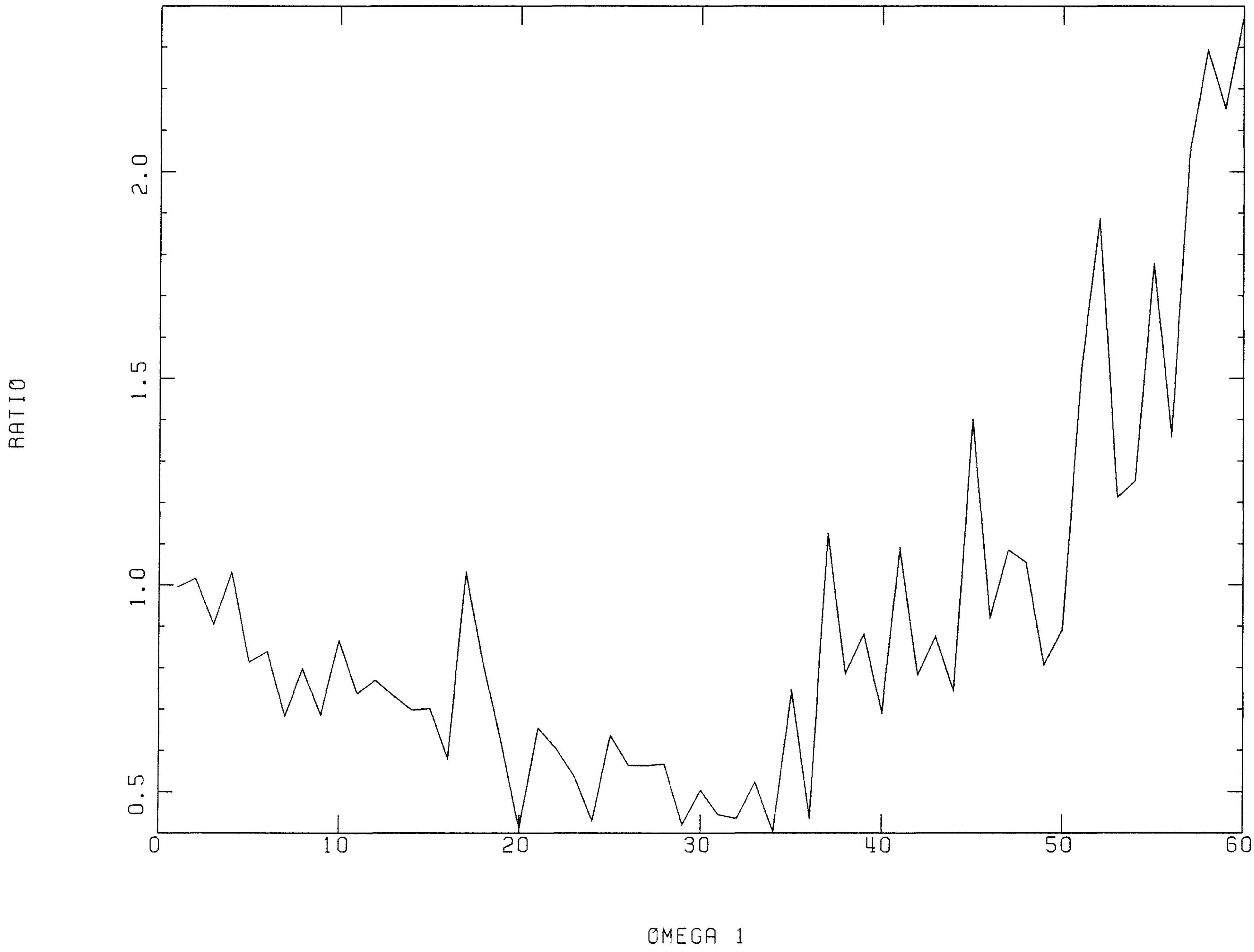

Fig 18

RHDIFF5-RHDIFF1, ØMEGA 2 = ØMEGA 1 DAMPING = 0.0, LENGTH = 30. SEC, CHANNEL 03

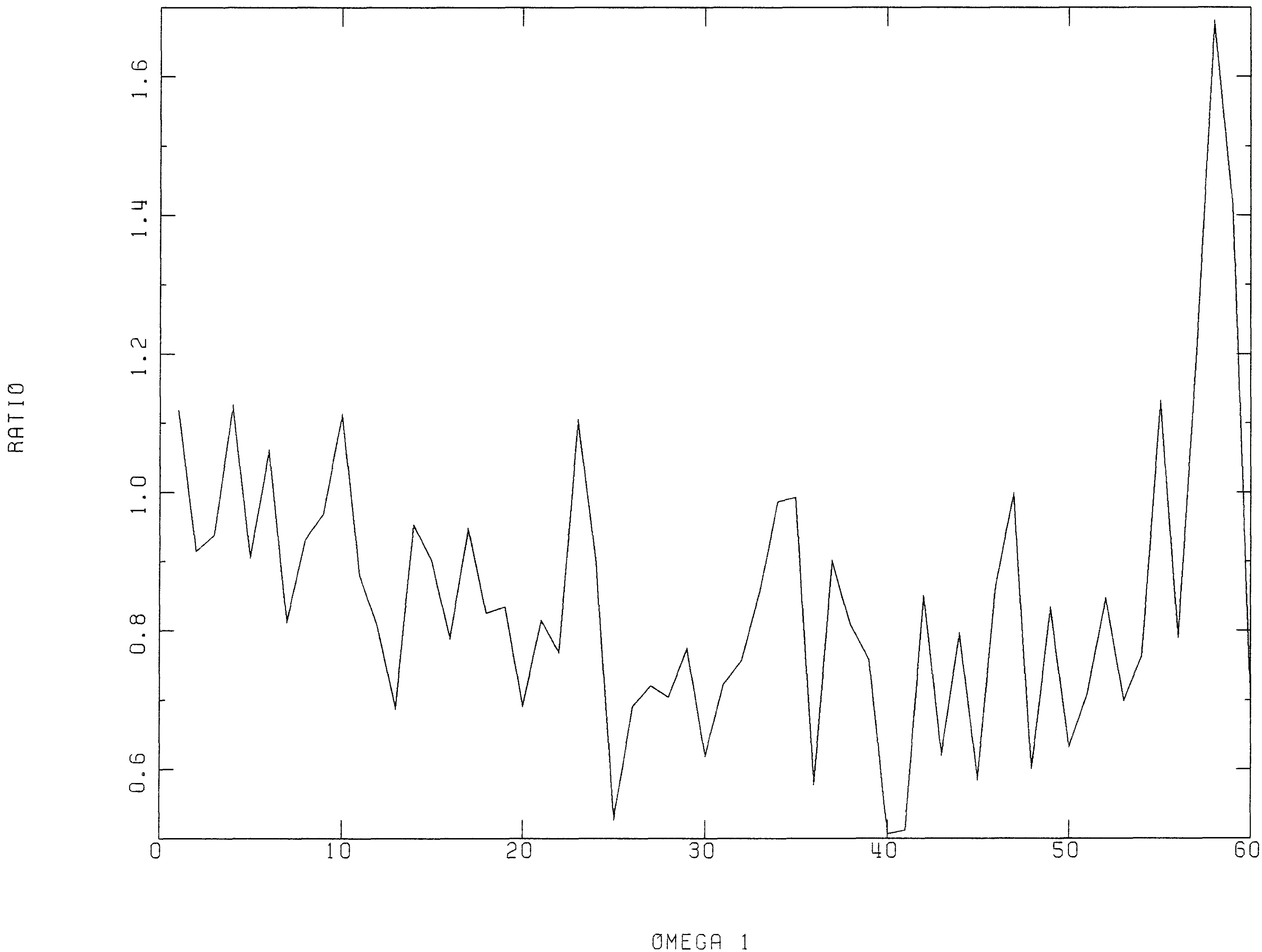

Fig. 19

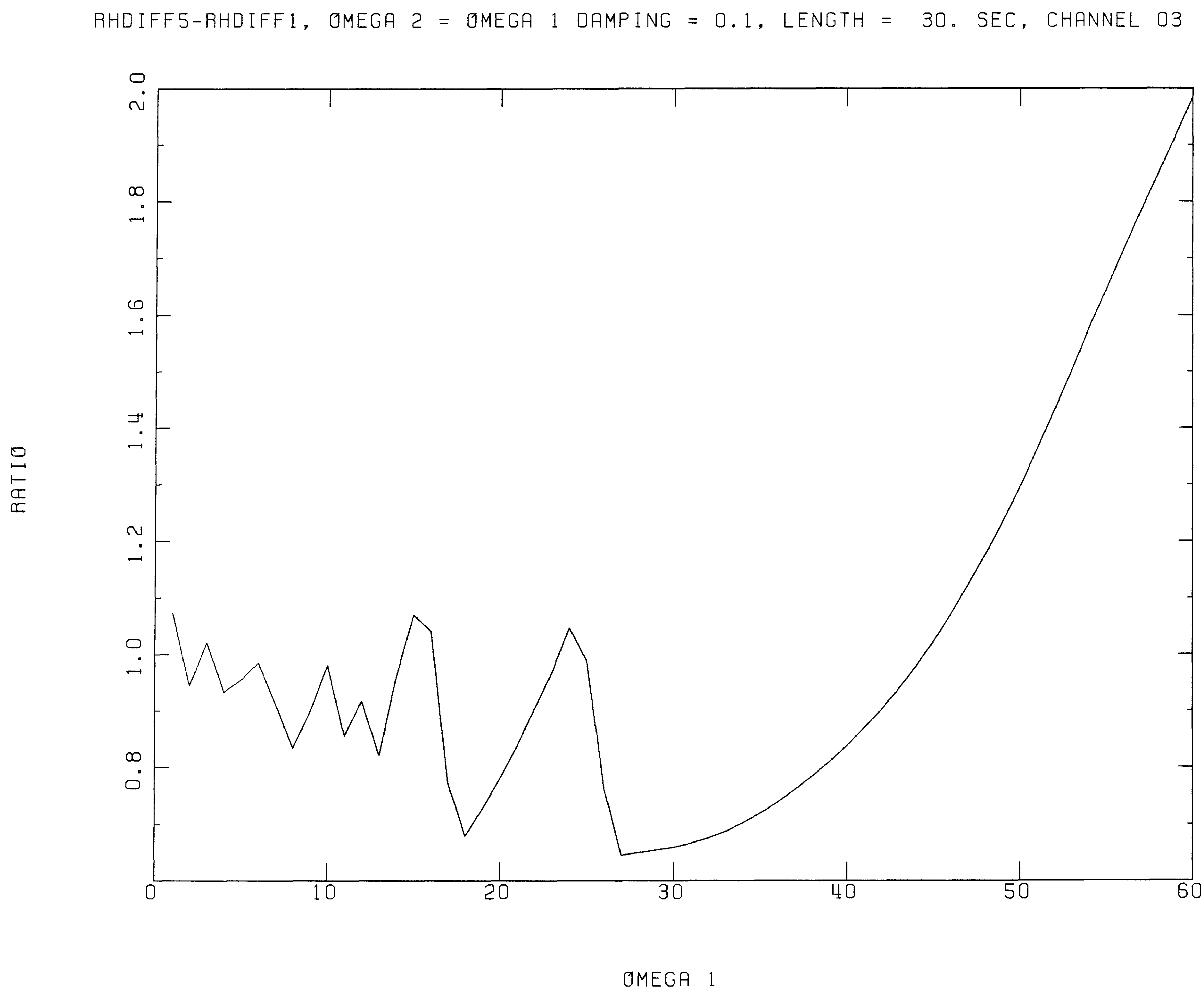
RHDIFF5-RHDIFF1, ØMEGA 2 = ØMEGA 1 DAMPING = 0.1, LENGTH = 30. SEC, CHANNEL 03
RATIØ
2.0
1.8
1.6
1.4
1.2
1.0
0.8
0
10
20
30
40
50
60
ØMEGA 1

Fig 20

RHDIFF5-RHDIFF1, ØMEGA 2 = ØMEGA 1 DAMPING = 0.2, LENGTH = 30. SEC, CHANNEL 03

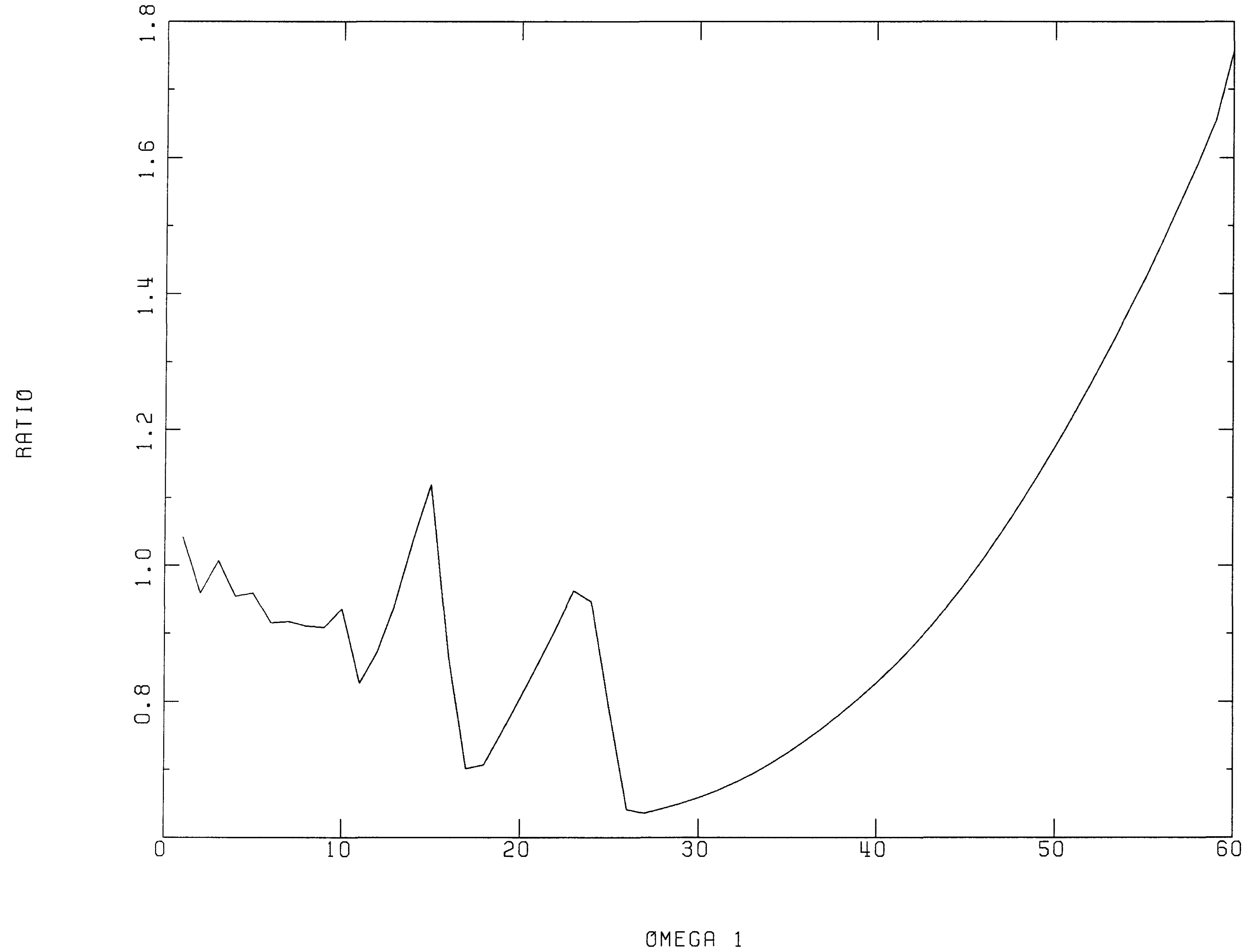

Fig 21

RHDIFF5-RHDIFF1, ØMEGA 2 = 10.0 DAMPING = 0.0, LENGTH = 30. SEC, CHANNEL 03

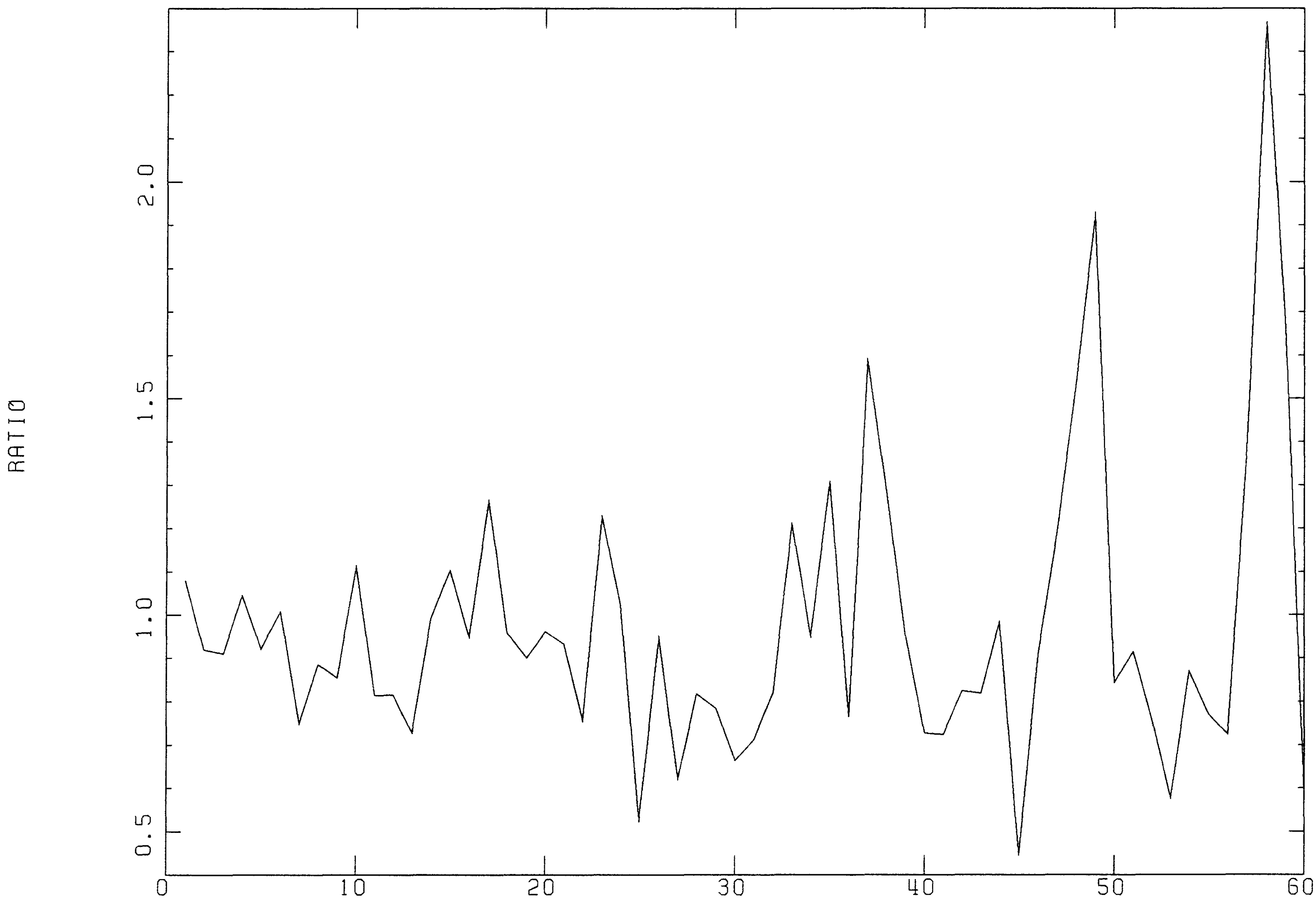

F 22

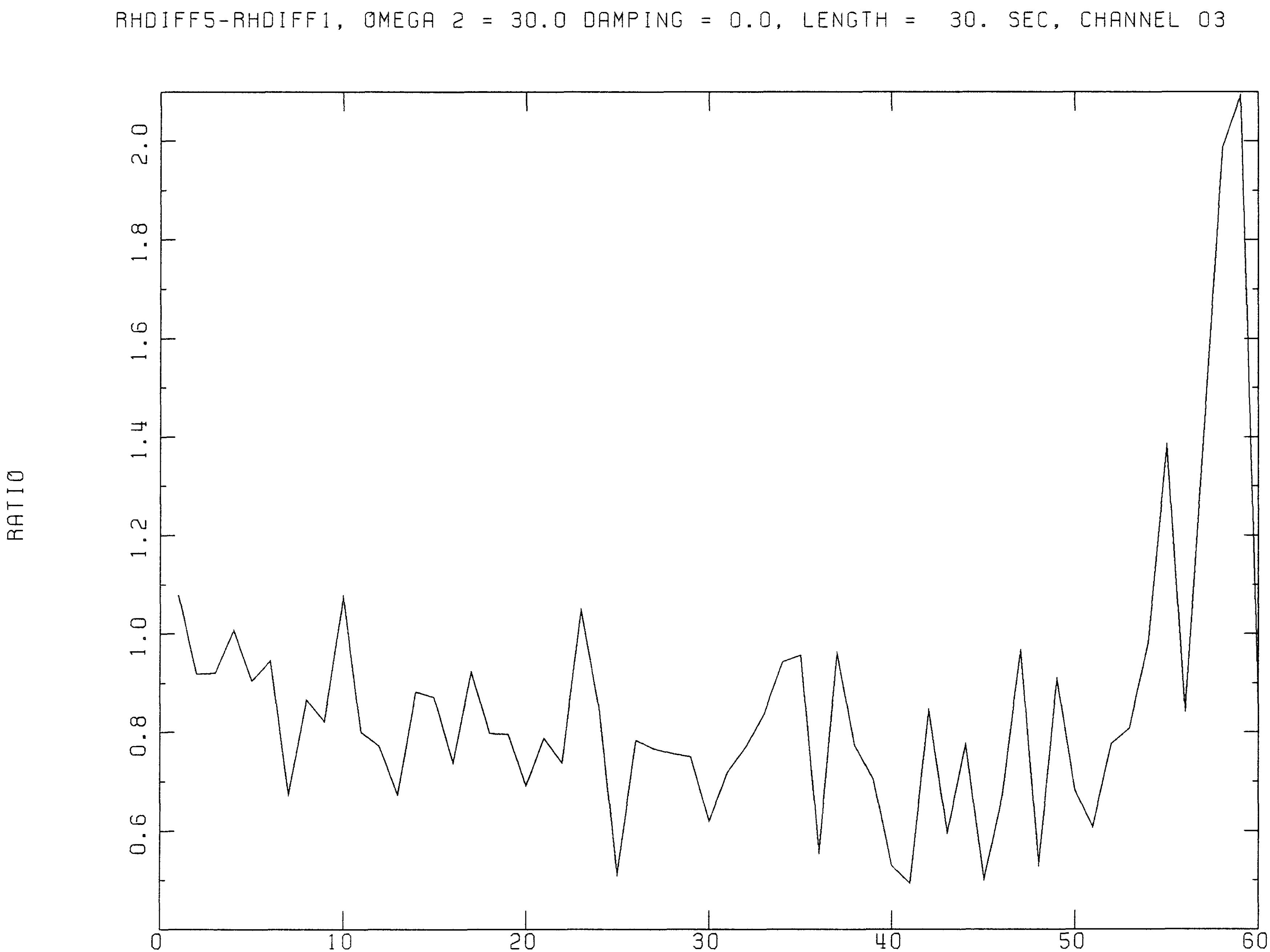

RHDIFF5-RHDIFF1, ØMEGA 2 = 30.0 DAMPING = 0.0, LENGTH = 30. SEC, CHANNEL 03
RATIO
0.6
0.8
1.0
1.2
1.4
1.6
1.8
2.0
0
10
20
30
40
50
60
ØMEGA 1

Fig 23

RHDIFF5-RHDIFF1, ØMEGA 2 = 50.0 DAMPING = 0.0, LENGTH = 30. SEC, CHANNEL 03

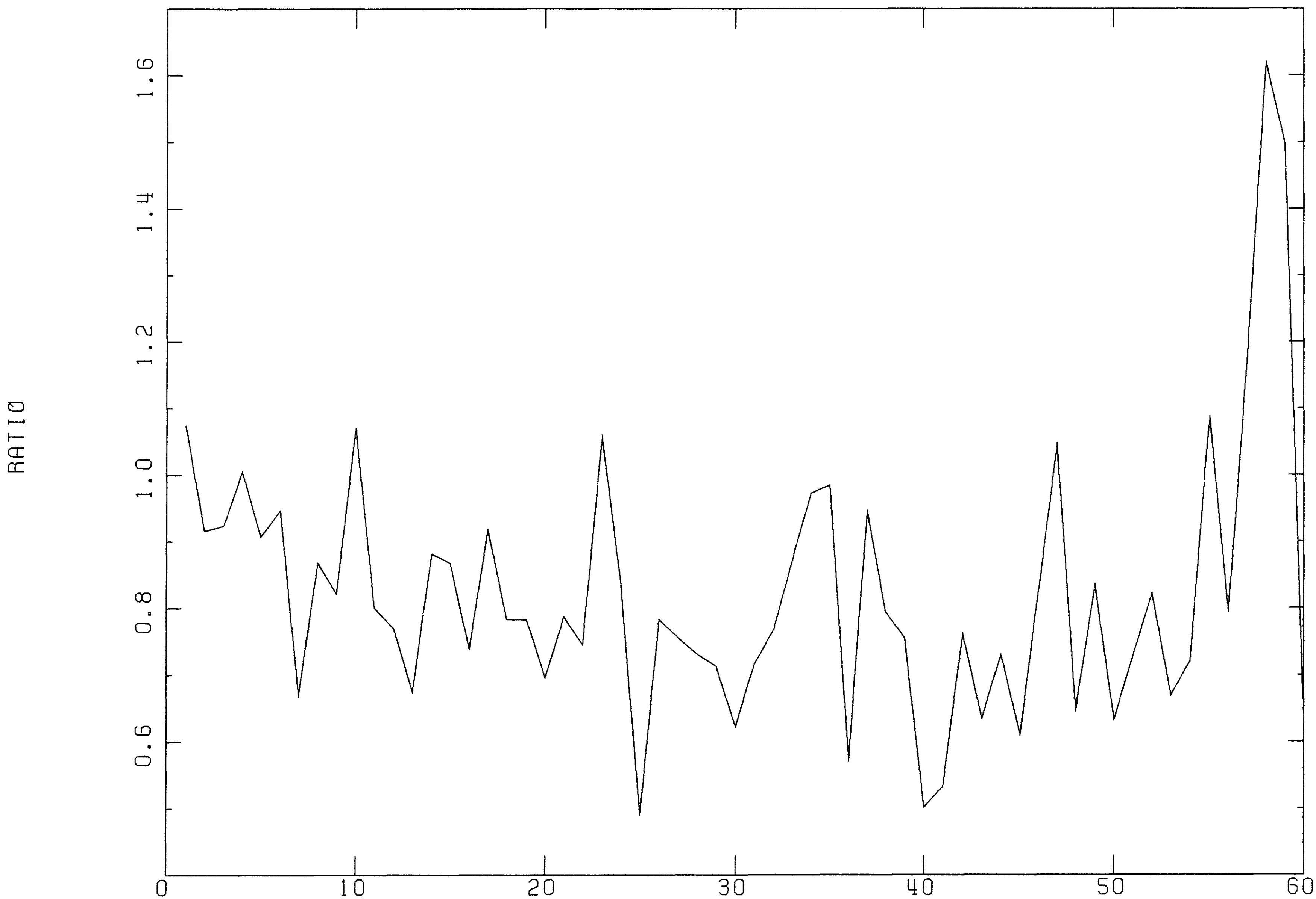

Fig 24

RHDIFF6-RHDIFF5, ØMEGA 2 = ØMEGA 1 DAMPING = 0.0, LENGTH = 30. SEC, CHANNEL 03

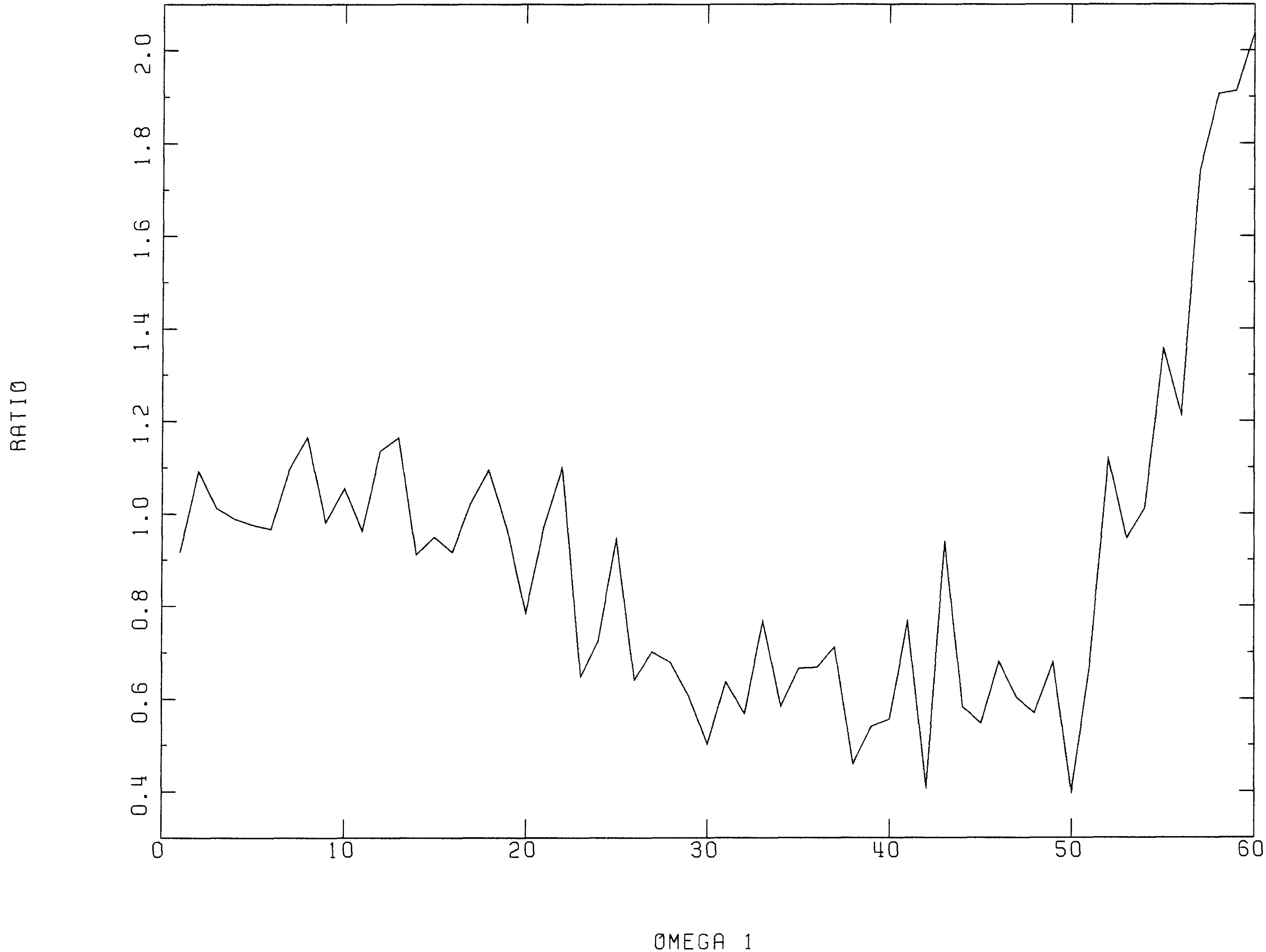

F[illegible] 25

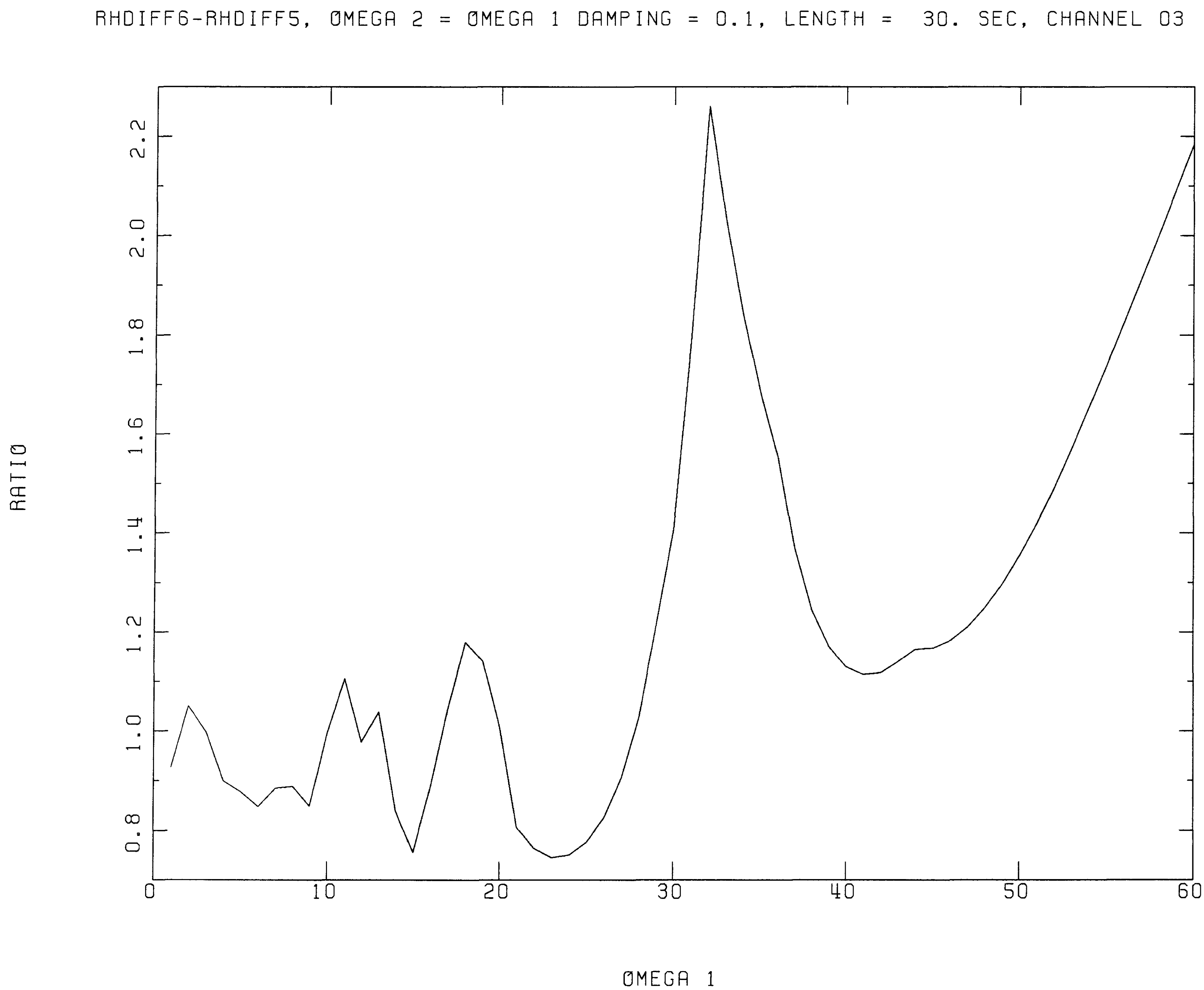
RHDIFF6-RHDIFF5, ØMEGA 2 = ØMEGA 1 DAMPING = 0.1, LENGTH = 30. SEC, CHANNEL 03
RATIO
0.8
1.0
1.2
1.4
1.6
1.8
2.0
2.2
0
10
20
30
40
50
60
ØMEGA 1

Fig 26

RHDIFF6-RHDIFF5, ØMEGA 2 = ØMEGA 1 DAMPING = 0.2, LENGTH = 30. SEC, CHANNEL 03

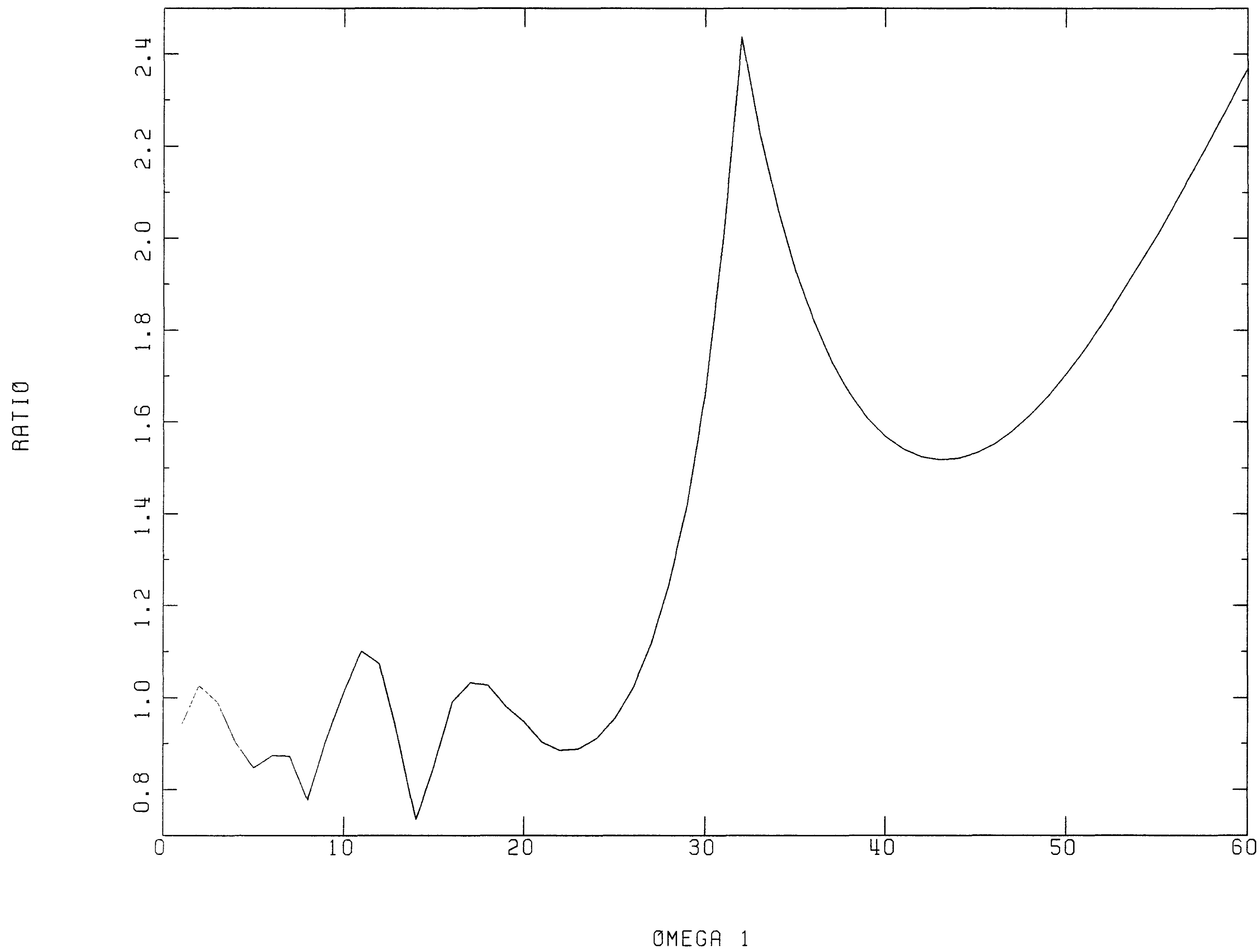

Fig 27

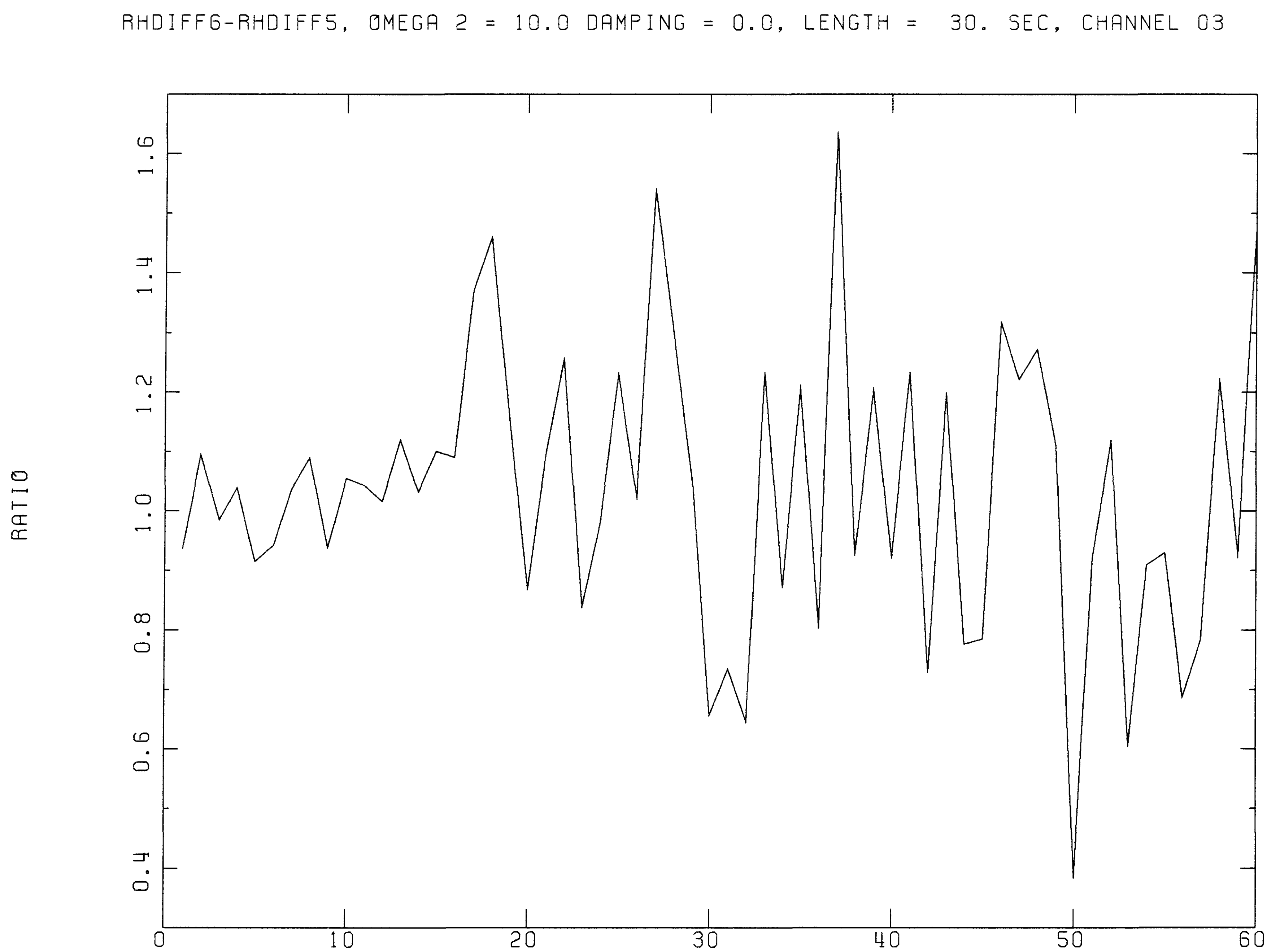
RHDIFF6-RHDIFF5, ØMEGA 2 = 10.0 DAMPING = 0.0, LENGTH = 30. SEC, CHANNEL 03
RATIØ
1.6
1.4
1.2
1.0
0.8
0.6
0.4
0
10
20
30
40
50
60
ØMEGA 1

Fig. 28

RHDIFF6-RHDIFF5, ØMEGA 2 = 30.0 DAMPING = 0.0, LENGTH = 30. SEC, CHANNEL 03

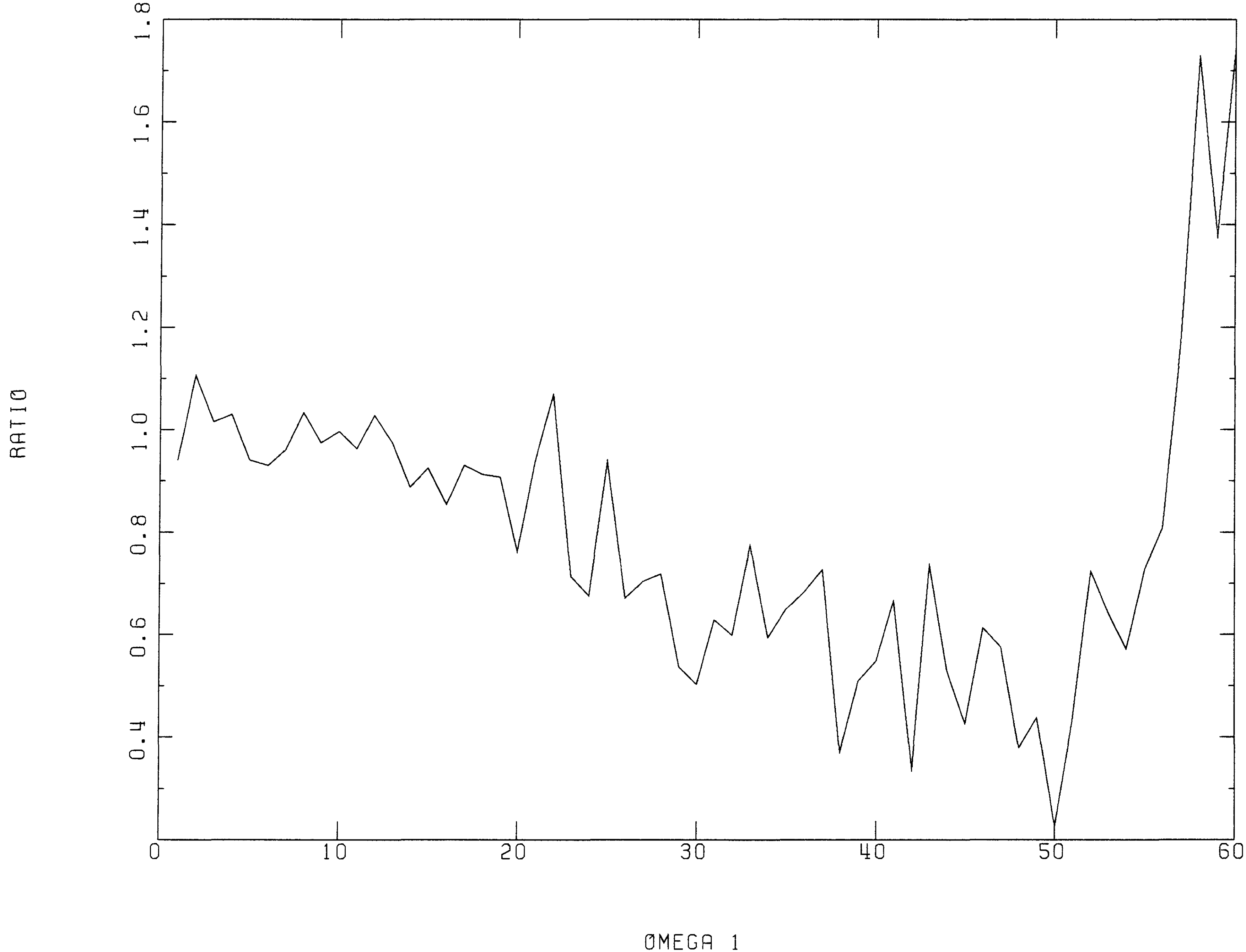

Fig 29

RHDIFF6-RHDIFF5, ØMEGA 2 = 50.0 DAMPING = 0.0, LENGTH = 30. SEC, CHANNEL 03

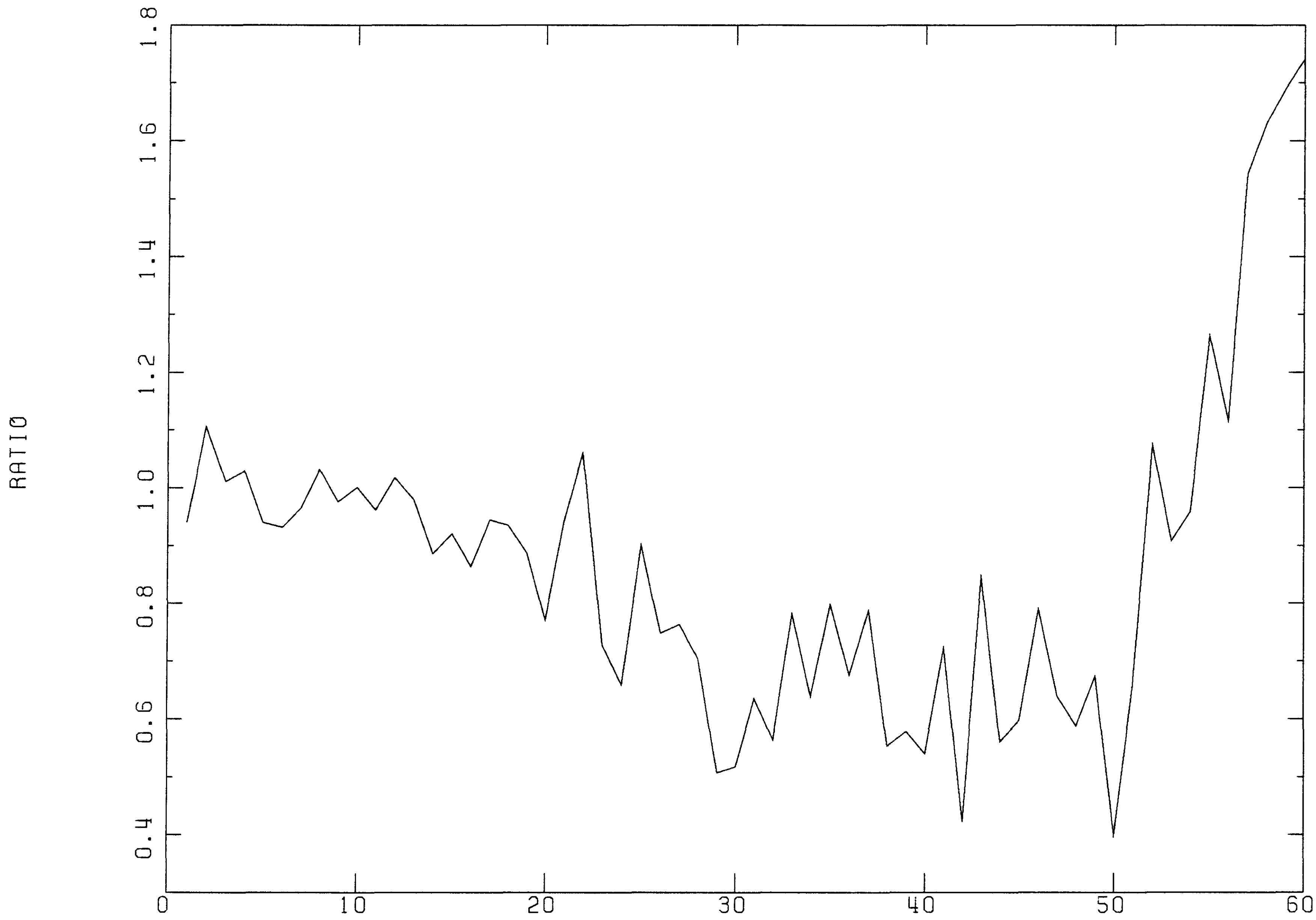

Fig 30